Engineering Journal

American Institute of Steel Construction

First Quarter 2013 Volume 50, No. 1

CELEBRATING 50 YEARS OF STEEL KNOWLEDGE

50

ENGINEERING JOURNAL

AMERICAN INSTITUTE OF STEEL CONSTRUCTION

Dedicated to the development and improvement of steel construction, through the interchange of ideas, experiences and data.

The articles contained herein are not intended to represent official attitudes, recommendations or policies of the Institute. The Institute is not responsible for any statements made or opinions expressed by contributors to this Journal.

The opinions of the authors herein do not represent an official position of the Institute, and in every case the officially adopted publications of the Institute will control and supersede any suggestions or modifications contained in any articles herein.

The information presented herein is based on recognized engineering principles and is for general information only. While it is believed to be accurate, this information should not be applied to any specific application without competent professional examination and verification by a licensed professional engineer. Anyone making use of this information assumes all liability arising from such use.

Manuscripts are welcomed, but publication cannot be guaranteed. All manuscripts should be submitted in duplicate. Authors do not receive a remuneration. A "Guide for Authors" is printed on the inside back cover.

ENGINEERING JOURNAL (ISSN 0013-8029) is published quarterly. Subscriptions: Members: one subscription, $40 per year, included in dues; Additional Member Subscriptions: $40 per year. Non-Members U.S.: $160 per year. Foreign (Canada and Mexico): Members $80 per year. Non-Members $160 per year. Published by the American Institute of Steel Construction at One East Wacker Drive, Suite 700, Chicago, IL 60601.

Periodicals postage paid at Chicago, IL and additional mailing offices. **Postmaster:** Send address changes to ENGINEERING JOURNAL in care of the American Institute of Steel Construction, One East Wacker Drive, Suite 700, Chicago, IL 60601.

Message from the Editor

Milestones have a way of catching you by surprise, such as when your car's odometer ticks over 100,000 miles or your parents reach a significant wedding anniversary (both of which occurred for me this past summer). I was equally caught by surprise by an *Engineering Journal* milestone: 2013 marks Volume 50 of the journal—our 50th year of publication.

AISC started *Engineering Journal* in 1964 as a means of communicating practical technical information to its membership. The first issue included articles from the great minds of Lev Zetlin (steel cables used to create "structural space systems"), T.R. Higgins (the then-new concept of effective length factors for columns) and Ted Galambos (lateral support to prevent sidesway buckling).

Back then, word processing as we know it didn't exist, and the phrase "cut and paste" referred to actions involving sharp blades, paper and glue. Inserting an image in a document involved cameras, film and lenses. This meant it was no easy feat to include large numbers of figures, drawings, photographs, sketches and equations, making the journal fairly advanced for the time.

Over the years *Engineering Journal* has expanded in scope to include coverage of contemporary steel research, but it continues to provide practical technical information reviewed by industry peers.

Here's to the next 50 years!

Keith A. Grubb

Keith A. Grubb, P.E., S.E.
Editor

Calculation of Stress Trajectories Using Fracture Mechanics

BO DOWSWELL

ABSTRACT

In structures composed of plates and plate-like elements subjected to in-plane stresses, the stress flow around discontinuities is an important design consideration. Stress dispersion angles are used extensively in gusset plate design and calculations for web local yielding of wide flange members. The current design values are empirical, and the variables affecting the dispersion angles are not well understood. Due to the wide range of angles published in the literature, an analytical model that accounts for all variables is necessary for full understanding of the behavior of these elements. Using fracture mechanics principles, this paper shows that the dispersion angle is dependent on geometry, constraint and inelastic deformation capacity. A versatile design procedure, which explicitly accounts for all variables affecting the stress dispersion angle, is presented.

Keywords: gusset plates, stress flow, discontinuities, fracture mechanics.

INTRODUCTION

In structures composed of plates and plate-like elements subjected to in-plane stresses, the stress flow around discontinuities is an important design consideration. A common discontinuity in steel-frame structures occurs where a concentrated load is dispersed into an element over a finite length. In a typical vertical brace connection, shown in Figure 1a, the brace axial load is dispersed into the gusset plate over the length of the brace-to-gusset connection. Another discontinuity is shown in Figure 1b, where the axial load in the post is transferred into the girder. To calculate the local strength of the girder web, the angle of dispersion within the girder must be estimated. The dispersion angle around openings in plate and shell structures must also be accurately predicted in order to calculate the proper development length of reinforcement and to estimate the net area at an offset group of openings.

The existing literature contains a wide range of experimental dispersion angles based on test results and finite element models. Researchers have reported angles as low as 16.1° and as high as 74°. Current design recommendations are limited to angles between 15° and 71.6°.

Due to the wide range of dispersion angles published in the literature, an analytical model that accounts for all of the variables affecting the stress dispersion angle is necessary for full understanding of the behavior of these elements. It will be shown that the dispersion angle is dependent on geometry, constraint and inelastic deformation capacity. This paper presents a versatile design solution, derived from the principles of fracture mechanics, that explicitly accounts for all variables affecting the stress dispersion angle.

Bo Dowswell, P.E., Ph.D., Principal, SDS Resources, LLC, Birmingham, AL. E-mail: bo@sdsresources.com

CURRENT DESIGN RECOMMENDATIONS

Design recommendations can be found in specifications, manuals, books and journal papers. In design, stress dispersion angles are used to determine an effective width of the element, where only a portion of the element is active in resisting the load.

Gusset Plates

For design, AISC (2011) treats gusset plates as rectangular, axially loaded members with a cross-sectional area $L_W t$, where L_W is the Whitmore width, and t is the plate thickness. The Whitmore width is calculated by assuming the stress spreads through the gusset plate at an angle of 30°. Whitmore widths are shown in Figure 2 for various connection configurations.

Web Local Yielding

This section discusses the local strength of members at concentrated loads located at the flanges and acting in the plane of the web. According to the AISC *Specification* (AISC, 2010) Section J10.2.a, web local yielding occurs when the web material adjacent to the fillet yields under a tensile or compressive force. When the concentrated force is applied at a distance from the member end greater than the depth of the member, the nominal load is

$$R_n = F_{yw}\, t_w \left(5k + l_b\right) \tag{1}$$

where

F_{yw} = specified minimum yield stress of the web, ksi
k = distance from outer face of flange to the web toe of the fillet, in.
l_b = length of bearing, in.
t_w = thickness of web, in.

The 2010 AISC *Specification* equations are based on a 2.5-to-1 slope from the load application point to the fillet as shown in Figure 3, which is a 68.2° dispersion angle. Eurocode (2005) Sections 6.2.6.2 and 6.2.6.3 have similar requirements, which are also based on a 68.2° dispersion angle.

For web yielding at end plate moment connections Eurocode (2005) specifies a 45° dispersion angle through the weld and the end plate and a 68.2° dispersion angle (2.5-to-1 slope) through the column flange and fillet radius. AISC Steel Design Guide 4 (Murray and Sumner, 2003) recommends a 45° dispersion angle through the weld and the end plate and a 71.6° dispersion angle (3-to-1 slope) through the column flange and fillet radius.

Plate and Shell Structures

Support points and openings for plate and shell structures are often reinforced with stiffening elements to prevent local

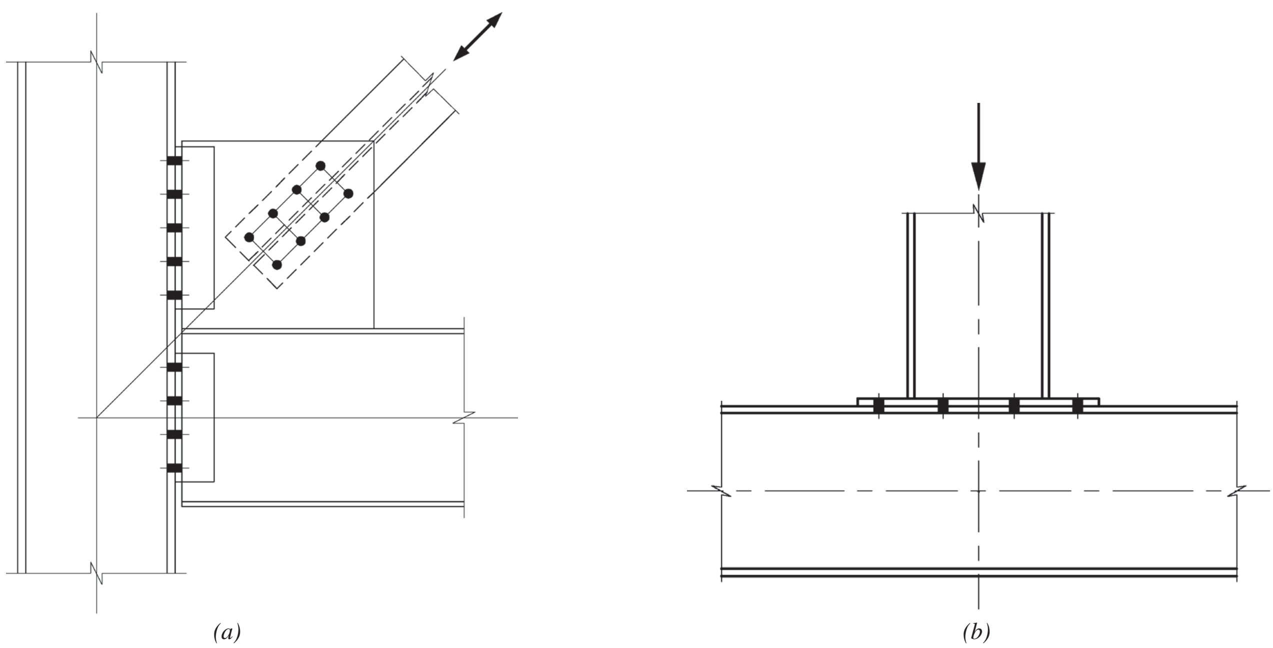

Fig. 1. Common discontinuities in steel-frame structures: (a) vertical brace connection; (b) post-to-girder connection.

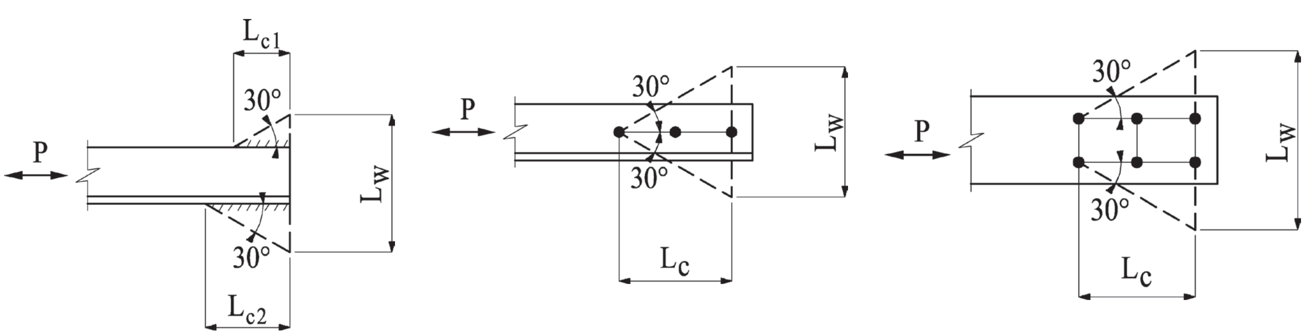

Fig. 2. Effective widths for various connection configurations.

yielding or buckling. The dispersion angle around openings must be accurately predicted in order to calculate the proper development length of reinforcement and to estimate the net area at an offset group of openings. Support members attached to the shell, such as the silo support in Figure 4, must be designed to properly disperse the stress into the shell to avoid buckling.

ASME *Steel Stack Code* (ASME, 2001) Section 4.6.1 states, "The top and bottom of the breeching opening shall be adequately reinforced to transfer the discontinuities of shell stress back to the full circumference of the shell." According to Commentary 5 of the CICIND *Model Code for Steel Chimneys* (CICIND, 1999), "Vertical reinforcement should be continued above and below the opening to a point where the added stress is unimportant. The code deems that continuing the reinforcement beyond horizontal stiffeners above and below the opening a distance at least 0.5 times the width of the opening will suffice." This implies a dispersion angle, θ, of 45° as shown in Figure 5.

Wolf (1983) discussed the design of silos at materials handling plants, and cited the transfer of load from the silo wall to the support columns as the most common cause of failure in these structures. He recommended that the loads be spread through the shell at an angle of 45°.

At locations of concentrated loads on steel tanks, Wozniak (1990) assumes the load to spread at an angle of 30° on each side of the stiffener as shown in Figure 6. The stiffener length is extended to a point where the stress in the shell is less than the allowable buckling stress. Wozniak also recommends that reinforcement be extended beyond openings far enough to allow a stress dispersion into the shell of 30°. Kaups and Lieb (1986) made similar recommendations for bins and silos.

For design of oil tanker structures with "several openings located in or adjacent to the same cross section," ABS (2009) Sections 2.6.3.6 and 2.6.3.8 specify an equivalent opening size based on a shadow area. The shadow area is calculated using "two tangent lines with an angle of 15 degrees to the longitudinal axis of the ship," as shown in Figure 7.

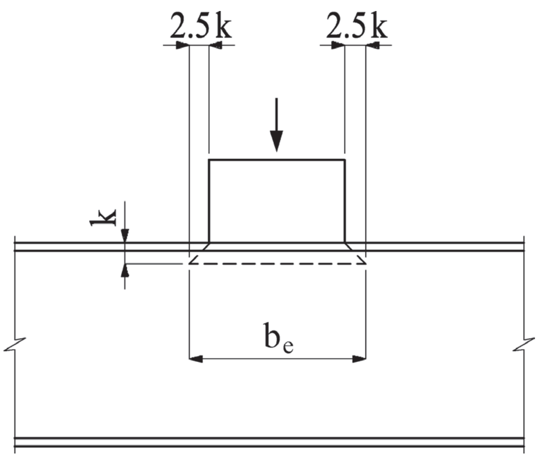

Fig. 3. Web local yielding.

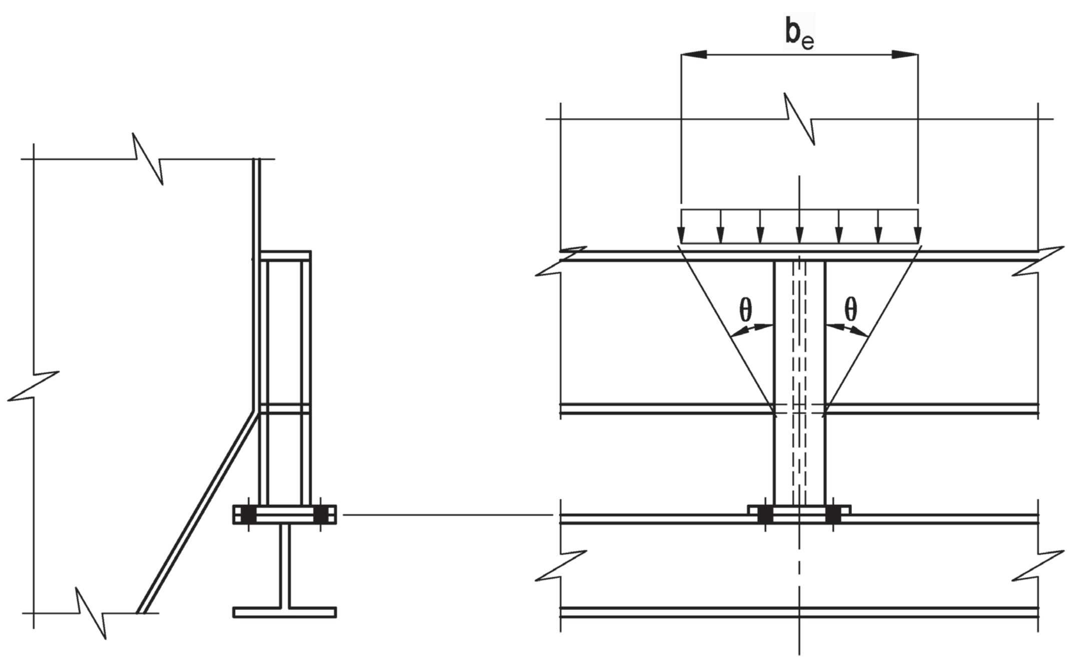

Fig. 4. Attachment to shell at discretely supported silo.

Connections

Owens and Cheal (1989) recommended dispersion angles of 30°, 45° and 68° for various conditions at steel connections, depending on the ductility of the fitting, boundary conditions and local symmetry.

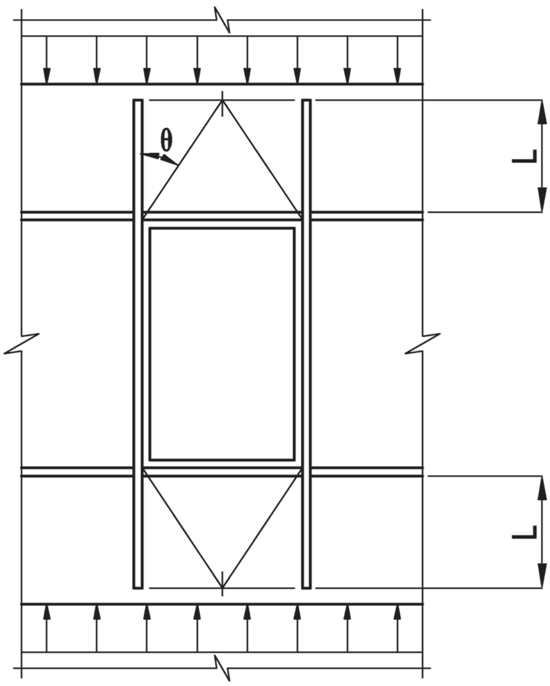

Fig. 5. Reinforced breech opening in a stack.

Crane Girders

The vertical normal stress in the web of a crane girder can be calculated by assuming that the wheel load disperses through the rail and top flange at an assumed angle, as shown in Figure 8. Ricker (1982) suggested an angle of 60°; however, a more conservative value of 45° has been adopted in CMAA (1994) Section 3.3.2.3, AS (2001) Section 5.7.3.3 and AISE (1997) Section 5.8.6.

EXISTING RESEARCH

Gusset Plates

The first major experimental work on gusset plates was done by Wyss (1923). The stress trajectories were plotted for gusset plate specimens representing a warren truss joint. The maximum normal stress was at the end of the brace member. Wyss noted that the stress trajectories were along approximately 30° lines with the connected member.

Sandel (1950) conducted a photoelastic stress analysis of a $^{1}/_{22}$-scale model of a Warren truss joint. The stress trajectories are shown in Figure 9a. He concluded that the normal stress at the end of the bracing members can be calculated more accurately using a stress trajectory angle of 35° instead of the 30° suggested by Wyss.

Whitmore (1952) tested ⅛-in.-thick aluminum gusset plates with a yield strength of 39 ksi and a modulus of elasticity of 10,000 ksi. The specimen was a 4-scale model of a Warren truss joint with double gusset plates. Data from strain gages mounted on the gusset plates were used to plot

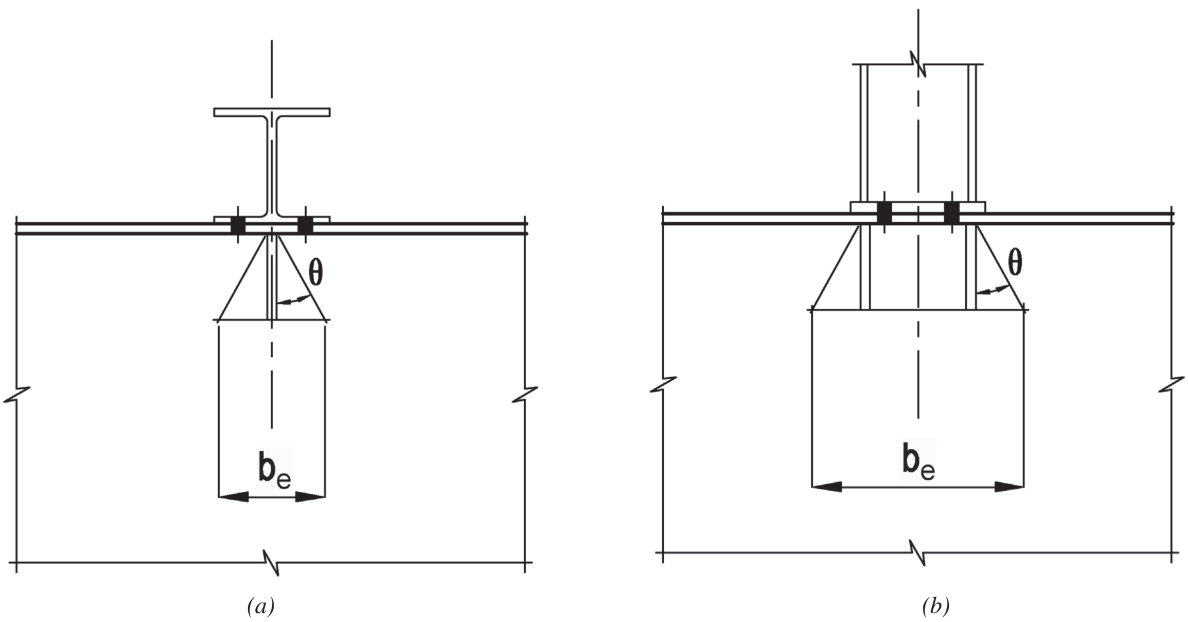

Fig. 6. Detail for concentrated load at the roof of a tank or silo: (a) single stiffener; (b) multiple stiffeners.

stress trajectories, which are shown in Figure 9b. These plots confirmed the work of Wyss (1923) and Sandel (1950), showing that the maximum normal stress was at the end of the members and the stress trajectories were along approximately 30° lines with the connected member.

Irvan (1957) tested a model of a Pratt truss joint with double gusset plates. The gusset plates were ⅛-in.-thick aluminum, with a yield strength of 35 ksi and a modulus of elasticity of 10,000 ksi. Data from strain gauges were used to plot the tension, compression and shear stresses in the gusset plate. The stress trajectories are shown in Figure 9c. Although the plots show a slightly wider dispersion angle than those of Wyss (1923), Sandel (1950) and Whitmore (1952), Irvan proposed that the 30° lines should project from the center of gravity of the rivet group instead of the outside fasteners on the first row. This gives an effective stress trajectory angle of 16.1° over the full fastener length.

Chesson and Munse (1963) tested 30 riveted and bolted truss connections with gusset plates. The specimens were loaded in tension until one of the components failed. The authors recommended that the normal stress at the end of bracing members be calculated using a stress trajectory angle of 22° for plates with punched holes and 25° for plates with drilled holes.

Yamamoto, Akiyama and Okumura (1985) investigated the stress distribution of eight Warren- and Pratt-type truss joints with double gusset plates. Test specimens were made of 8-mm (0.315-in.)-thick gusset plates. They plotted the stress distribution using data from strain gauges mounted on the gusset plates. The researchers used the finite element method to perform an inelastic analysis on the plates. They found that "the plastic region, which appears in the inner part of the gusset plate at the earlier loading stage, develops toward the outer part with the load increasing." Using the results of "numerical evaluations of a great variety of bolt arrangements," the researchers proposed a dispersion angle of 22°.

Cheng and Grondin (1999) summarized the research on gusset plates loaded in compression at the University of Alberta. They noted that yielding in the specimens allowed the stress to redistribute and recommended a 45° dispersion angle. Using an equivalent column method to calculate the buckling strength with a 45° dispersion angle, the nominal strengths agreed well with the test results.

Additional research on gusset plates by Lavis (1967), Rabern (1983), Chakrabarti (1983), Bjorhovde and Chakrabarti (1985), Gross and Cheok (1988), and Girard, Picard and Fafard (1995) verified 30° stress trajectories.

Web Local Yielding

The equations for web local yielding in the 1937 AISC *Specification* (AISC, 1937) are based on a 45° dispersion angle from the load application point to the fillet, as shown in Figure 10. Based on nine tests of directly welded moment connections to column flanges, Sherbourne and Jensen (1957) showed that the 45° dispersion angle is overly conservative. They proposed a 63.4° dispersion angle (2-to-1 slope) for design.

Graham, Sherbourne, Khabbaz and Jensen (1959) tested 11 specimens that simulated the column near a compression flange in a directly welded moment connection. Yielding of the web initiated beneath the load, and the width of the yielded region became wider as the load increased. The specimens failed by buckling after significant yielding of the web. All of the test loads exceeded the nominal strength predicted using a dispersion angle of 74.0° (3.5-to-1 slope).

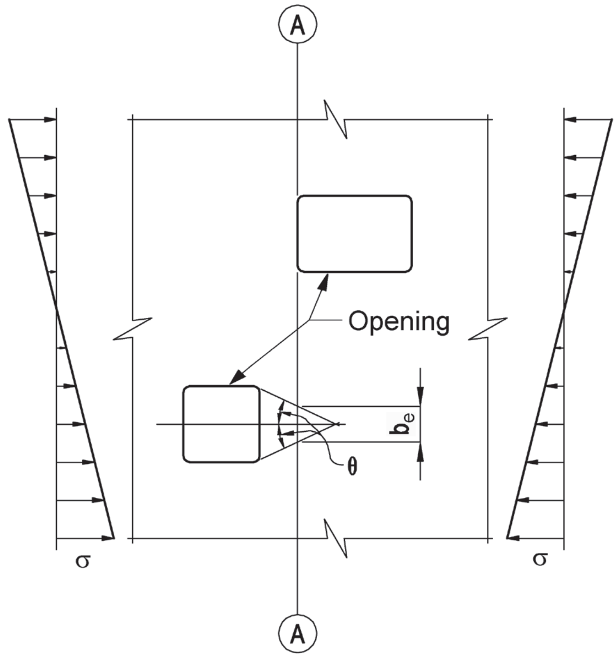

Fig. 7. Equivalent opening size.

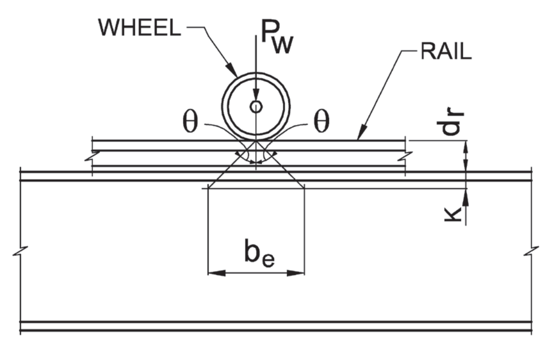

Fig. 8. Crane girder with a concentrated wheel load.

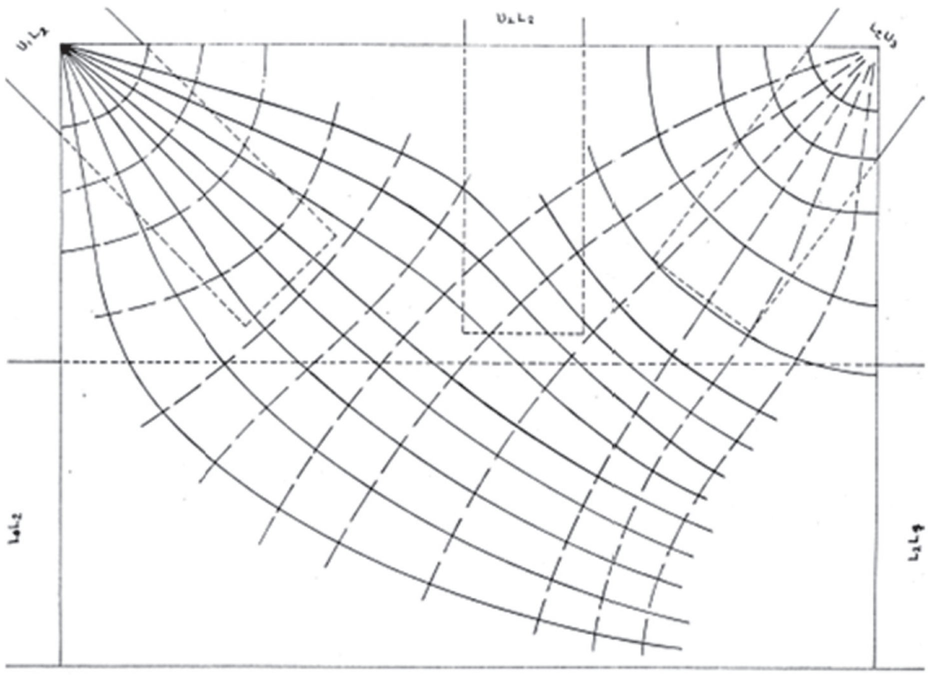

Fig. 9a. Experimental stress trajectories in gusset plates, Sandel (1950).

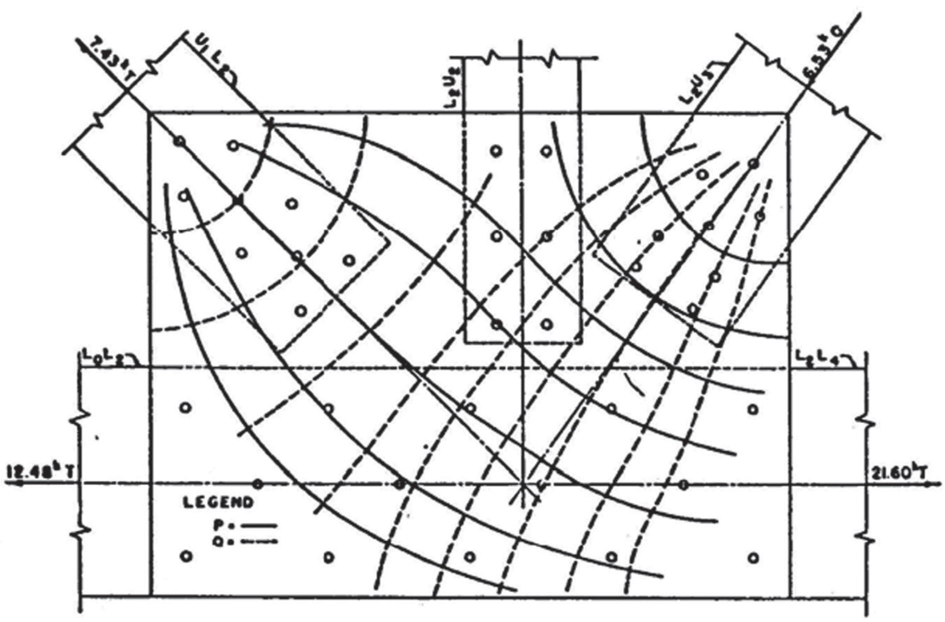

Fig. 9b. Experimental stress trajectories in gusset plates, Whitmore (1952).

The authors recommended a conservative dispersion angle of 68.2° (2.5-to-1 slope) for design purposes; however, they also presented a plastic analysis approach, where they recommended a dispersion angle of 74.0° (3.5-to-1 slope).

Based on experimental tests and numerical models, Aribert, Lauchal and Nawawy (1981) proposed three equations based on the magnitude of the load. At the maximum elastic load, they recommended an effective width of $t_p + 2.3k$, which is equivalent to a 26.6° dispersion angle through the end plate and a 49.0° dispersion angle through the column. At the maximum plastic load, they proposed an effective width of $2t_p + 5k$, which is equivalent to a 45° dispersion

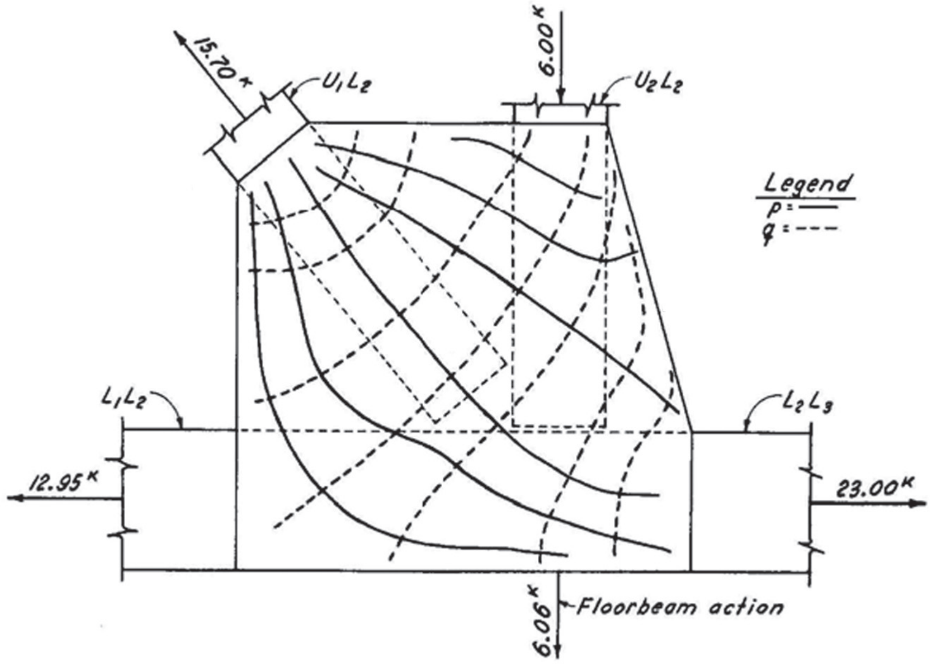

Fig. 9c. Experimental stress trajectories in gusset plates, Irvan (1957).

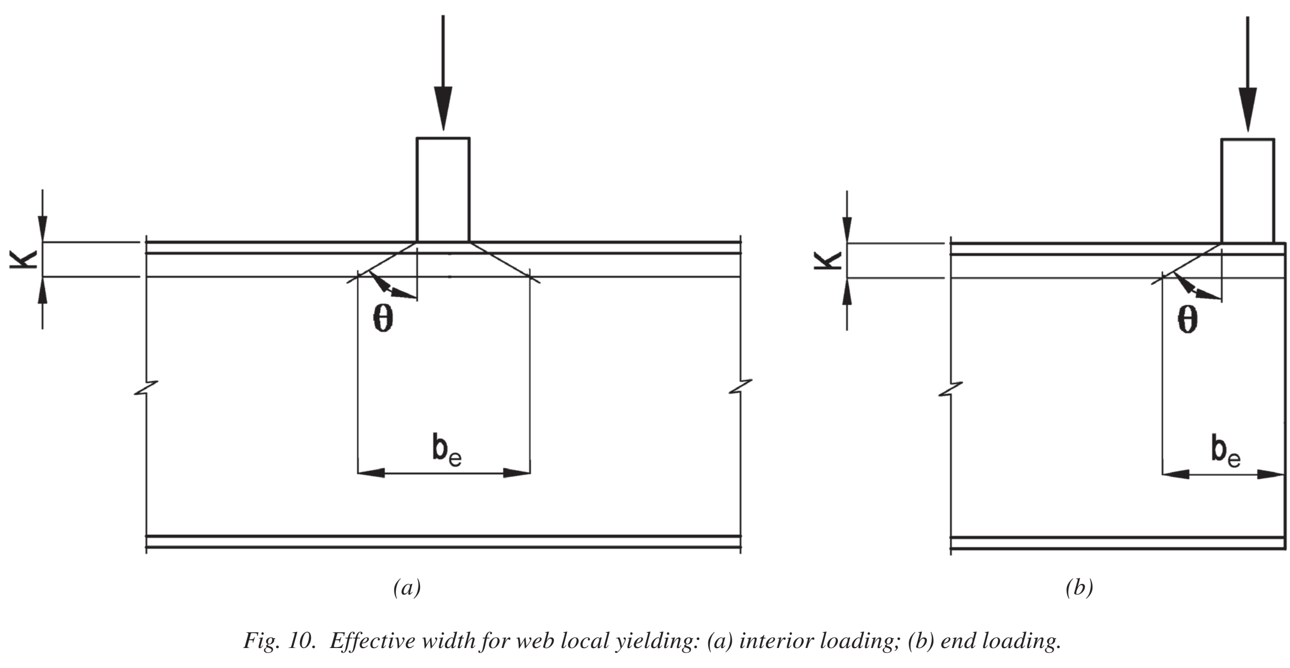

Fig. 10. Effective width for web local yielding: (a) interior loading; (b) end loading.

angle through the end plate and a 68.2° dispersion angle through the column. At the ultimate load, the recommended effective width is $6t_p + 7k$, which is equivalent to a 71.6° dispersion angle through the end plate and a 74.0° dispersion angle through the column.

Based on inelastic finite element models and six experimental tests on end plate moment connections, Hendrick and Murray (1983) recommended a 45° dispersion angle through the weld and the end plate and a 71.6° dispersion angle (3-to-1 slope) through the column. These recommendations are also included in AISC Steel Design Guide 4 (Murray and Sumner, 2003). The tests and finite element models clearly showed that the dispersion angle increased with load, especially after the yield strain was exceeded.

Beam Webs

Young and Hancock (2000) tested a series of cold-formed channels with local compression loads in the plane of the web. They found that the dispersion angle through the web was greater for interior loading than for end loading. For members loaded at both flanges, the authors recommended dispersion angles of 54.5° and 31.0° for interior loading and end loading, respectively. For members loaded at only one flange, they recommended dispersion angles of 52.4° and 45.0° for interior loading and end loading, respectively.

Plate and Shell Structures

The finite element models of Wang (1974), Gould, Sen, Wang, Suryoutomo and Lowery (1976), and Zhao and Yu (2005) were used to study the behavior of discretely supported silos and tanks. As expected, the models showed that the compressive stress in the shell was much higher above the supports, and the buckling strength of the shell increased with the engagement length of the columns. Pasternak (2002) discussed two silos with discrete supports that failed in service due to local buckling of the shell directly above the support. He concluded that the stresses in the shell directly above the support were too high due to insufficient stiffener length.

Shear Lag

Abi-Saad and Bauer (2006) used an effective width approach with a dispersion angle of 30° to calculate the reduced strength of members due to the effects of shear lag.

General Observations

Young and Hancock (2000) showed that the element geometry affects the dispersion angle. When the member is loaded at the end, the average suggested dispersion angle is only 71% of the average value for interior loading.

The effect of constraint can be observed by comparing the gusset plate tests to the local web yielding tests. The test results showed dispersion angles of 22° to 45° for gusset plates and 49° to 74° for local web yielding. Gusset plates are plane stress elements, but the elements in local web yielding calculations are restrained by the beam flange in both directions perpendicular to the load.

Experimental observations of Graham et al. (1959), Aribert et al. (1981), Hendrick and Murray (1983), Yamamoto et al. (1985) and Cheng and Grondin (1999) showed that the stress dispersion angle increases with inelastic material behavior.

FRACTURE MECHANICS APPROACH

Fracture mechanics solutions are available for a wide range of loading conditions and crack geometries. Although cracks do not exist in the elements that are the subject of this paper, fracture mechanics can be used to determine the stress field adjacent to any discontinuity. The stress-trajectory angle around the discontinuity can be determined using the energy release rate of an equivalent crack.

Basic Solution

Bažant and Cedolin (1991) described a stress relief zone, which is a stress-free zone in the material ahead of a crack as shown in Figure 11. Their derivation, which used principles of fracture mechanics to determine the stress dissipation angle, is shown here. They assumed a region of zero stress to be bounded by lines of constant slope, k_s. The strain energy per unit thickness for a crack length $2a$ is

$$\Delta U = -2k_s a^2 u \tag{2}$$

The strain energy density is

$$u = \frac{\sigma^2}{2E} \tag{3}$$

The energy release rate on each side of the crack centerline is

$$\begin{aligned} W &= \frac{-\mathrm{d}\Delta U}{\mathrm{d}a} \\ &= \frac{2k_s a \sigma^2}{E} \end{aligned} \tag{4}$$

From Irwin (1957), the energy release rate per crack tip is

$$G = \frac{K_I^2}{E} \tag{5}$$

The critical stress intensity factor for a crack in an infinitely wide plate in tension is

$$K_I = \sigma\sqrt{\pi a} \tag{6}$$

Equation 6 is substituted into Equation 5 to get

$$G = \frac{\pi\sigma^2 a}{E} \tag{7}$$

Because W must equal G, Equation 4 is set equal to Equation 7 and solved for k_s. The slope of the stress dispersion line is

$$k_s = \frac{\pi}{2} \tag{8}$$

where
- E = modulus of elasticity, ksi
- G = energy release rate per crack tip, kip-in.
- K_I = stress intensity factor, ksi-in.$^{1/2}$
- ΔU = strain energy per unit thickness, kips
- W = energy release rate on each side of the crack centerline, kip-in.
- a = half crack length, in.
- k_s = slope of the stress dispersion line
- u = strain energy density, ksi
- σ = applied axial stress, ksi

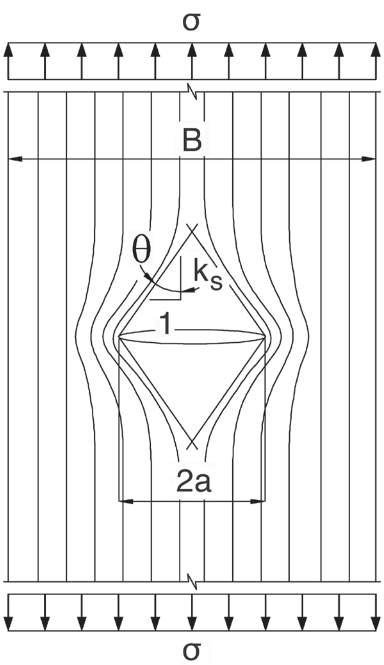

Fig. 11. Stress-free zone ahead of a crack.

This is equivalent to a dispersion angle of 32.5°, which is in reasonable agreement with the experimental results for elastic gusset plates. However, a general design solution must account for the element geometry, the effect of constraint and inelastic material behavior.

Effect of Element Geometry

The stress intensity factor is dependent on the element geometry, crack size, load level and loading configuration. In this paper, the elements will be loaded only in axial tension, and the only two element geometries will be considered: center crack tension (CCT) and single-edge notch tension (SENT). These are illustrated in Figure 12.

The stress intensity factor equations for cracks in infinitely wide plates are (Broek, 1986)

CCT

$$K_I = \sigma\sqrt{\pi a} \tag{9}$$

SENT

$$K_I = \beta\sigma\sqrt{\pi a} \tag{10}$$

where $\beta = 1.12$ is the free-surface correction factor.

Effect of Constraint

The strain energy density is the strain energy per unit volume, which is calculated as the area under the stress-strain curve. Equation 3 is applicable only to elastic materials in uniaxial tension. Cook and Young (1985) and Chen and Han (1988) showed the derivation of Equation 3.

$$\begin{aligned} u &= \int_0^{\varepsilon} \sigma\, d\varepsilon \\ &= \frac{\sigma\varepsilon}{2} \\ &= \frac{\sigma^2}{2E} \end{aligned} \tag{11}$$

For plane stress with no shear component, the strain energy density is

$$u = \int_0^{\varepsilon_{ij}} \sigma_{ij} d\varepsilon = \frac{1}{2E}\left(\sigma_x^2 + \sigma_y^2 - 2\upsilon\sigma_x\sigma_y\right) \tag{12}$$

And for three-dimensional stress with no shear component,

$$u = \int_0^{\varepsilon_{ij}} \sigma_{ij} d\varepsilon = \frac{1}{2E}\left[\sigma_x^2 + \sigma_y^2 + \sigma_z^2 - 2\upsilon\left(\sigma_x\sigma_y + \sigma_y\sigma_z + \sigma_z\sigma_x\right)\right] \tag{13}$$

where
- ν = Poisson's ratio
- ε_{ij} = strain tensor
- σ_{ij} = stress tensor
- σ_x = normal stress in the x direction, ksi
- σ_y = normal stress in the y direction, ksi
- σ_z = normal stress in the z direction, ksi

For states of stress with an applied load in the x-direction and constraint in the y- and z-directions, Blodgett (1998) derived Equations 14 and 15 to determine σ_y and σ_z normal stresses due to the constraint.

$$\sigma_y = \sigma_x\,(0.330C_y + 0.0989C_z) \tag{14}$$

$$\sigma_z = \sigma_x\,(0.0989C_y + 0.330C_z) \tag{15}$$

where
- C_y = factor for restraint in the y-direction
- C_z = factor for restraint in the z-direction

For plane stress conditions with an applied stress in the x-direction and rigid constraint in the y-direction, $C_y = 1.0$ and $C_z = 0$. When these values are substituted into Equations 14 and 15, the constraint stresses are

$$\sigma_y = 0.330\sigma_x \tag{16}$$

$$\sigma_z = 0.0989\sigma_x \tag{17}$$

If Equations 16 and 17 are substituted into Equation 13, with $\nu = 0.3$, the resulting strain energy density is

$$u = 0.421\frac{\sigma_x^2}{E} \tag{18}$$

For conditions with rigid constraint in the y- and z-directions, $C_y = 1.0$ and $C_z = 1.0$. When these values are substituted into Equations 14 and 15, the constraint stresses are

$$\sigma_y = 0.429\sigma_x \tag{19}$$

$$\sigma_z = 0.429\sigma_x \tag{20}$$

If Equations 19 and 20 are substituted into Equation 13, the resulting strain energy density is

$$u = 0.371\frac{\sigma_x^2}{E} \tag{21}$$

Another effect of the multi-axial state of stress is the higher effective yield stress of the material. Using von Mises' equation, the effective stress is (Boresi, Schmidt and Sidebottom, 1993).

$$\sigma_e = \sqrt{\frac{1}{2}\left[\left(\sigma_x - \sigma_y\right)^2 + \left(\sigma_y - \sigma_z\right)^2 + \left(\sigma_z - \sigma_x\right)^2\right]} \tag{22}$$

To determine the effective yield stress in the x-direction for conditions with rigid constraint in one direction, σ_y and σ_z from Equations 16 and 17 are substituted into Equation 22.

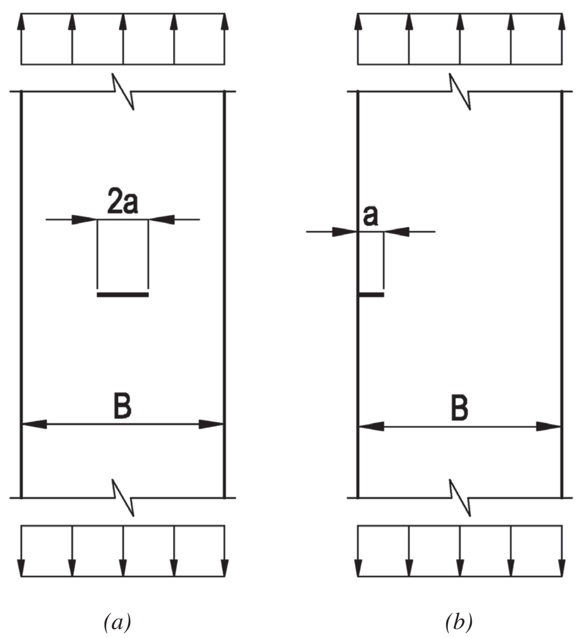

Fig. 12. Element geometry: (a) CCT; (b) SENT.

And then, Equation 22 is solved for σ_x. At yield, σ_e is equal to the uniaxial yield strength, F_y, and σ_x is equal to the effective yield stress in the x-direction, F'_y. These substitutions result in Equation 23.

$$F'_y = 1.23F_y \tag{23}$$

For rigid constraint in two directions, Equations 19 and 20 are substituted into Equation 22, which results in Equation 24.

$$F'_y = 1.75F_y \tag{24}$$

The x-direction strain is determined from Equation 25 (Cook and Young, 1985).

$$\varepsilon_x = \frac{1}{E}\left[\sigma_x - \upsilon\left(\sigma_y + \sigma_z\right)\right] \tag{25}$$

Equations 14 and 15 are substituted into Equation 25 to get Equation 26.

$$\varepsilon_x = \frac{\sigma_x}{E}\left[1 - 0.129\left(C_y + C_z\right)\right] \tag{26}$$

Inelastic Material Behavior

Based on linear-elastic perfectly plastic material behavior, the strain energy density for conditions of uniaxial stress with strains exceeding the yield strain is

$$u = F_y\left(\varepsilon - \frac{\varepsilon_y}{2}\right) \tag{27}$$

For multi-axial stress, the strain energy density is

$$u = F'_y\left(\varepsilon - \frac{\varepsilon'_y}{2}\right) \tag{28}$$

where

$$\varepsilon'_y = \frac{F'_y}{E}\left[1 - 0.129\left(C_y + C_z\right)\right] \tag{29}$$

ε_y = uniaxial yield strain
ε'_y = effective yield strain accounting for constraint

The stress intensity factor is a measure of the stress singularity at the crack tip. It is valid only in linear-elastic fracture mechanics (LEFM), which allows only small-scale yielding at the crack tip. Therefore, in the inelastic range, the accuracy of the LEFM solution degrades with increased inelasticity and elastic-plastic fracture mechanics (EPFM) must be used.

To estimate the effect of inelastic material behavior, Smith and Pilkington (1978) discussed the possibility of calculating a critical K_I value based on a J-integral solution, which was originally developed by Rice (1968) to characterize the fracture in nonlinear elastic materials. Elastic-plastic estimation procedures were developed by Shih and Hutchinson (1976), who proposed that the elastic-plastic J-integral value could be estimated as the sum of the elastic and plastic components:

$$J = J_e + J_p \tag{30}$$

The elastic value, J_e, is equal to Griffith's energy release rate, G (Griffith, 1920).

$$J_e = G \tag{31}$$

Irwin (1957) showed that, for conditions of plane stress,

$$\begin{aligned} G &= \frac{K_I^2}{E} \\ &= \frac{\pi\beta^2\sigma^2 a}{E} \end{aligned} \tag{32}$$

The value for K_I should be calculated with the effective crack size (Irwin, 1957), which is larger than the actual crack size due to the plastic zone adjacent to the crack tip. The modified Irwin plastic zone correction factor proposed by Kumar, German and Shih (1981) is

$$\begin{aligned} a_e &= a + \frac{1}{1+\left(P/P_0\right)^2}\left(\frac{1}{2\pi}\right)\left(\frac{n-1}{n+1}\right)\left(\frac{K_I}{\sigma_0}\right)^2 \\ &= a\left[1 + \frac{\left(\sigma/\sigma_0\right)^2}{1+\left(\sigma/\sigma_0\right)^2}\left(\frac{\beta^2}{2}\right)\left(\frac{n-1}{n+1}\right)\right] \end{aligned} \tag{33}$$

He and Hutchinson (1983) derived the fully plastic J-integral solution for semi-infinite plates with a crack at the center.

$$J_p = \pi\sqrt{n}\,\frac{k\varepsilon_0 a}{\sigma_0^n}\sigma^{n+1} \tag{34}$$

where n and k are Ramberg-Osgood coefficients (Ramberg and Osgood, 1943) for the true stress-strain curve. The Ramberg-Osgood equation is

$$\frac{\varepsilon}{\varepsilon_0} = \frac{\sigma}{\sigma_0} + k_r \left(\frac{\sigma}{\sigma_0}\right)^n \tag{35}$$

where σ_0 and ε_0 are usually set equal to the yield stress and yield strain, respectively. Variables n and k_r are determined empirically, based on the true stress-strain curve for the material in question. Values based on best-fit curve fitting to data in NIST (2005) are:

$k_r = 2.4$ and $n = 5.8$ for ASTM A36 steel
$k_r = 1.8$ and $n = 7.4$ for ASTM A572 Grade 50 steel

Equations 30 through 35 can be used to determine an effective J-integral solution; however, this results in a very complicated, iterative solution that can be simplified for design purposes into Equation 36.

$$J = \lambda G \tag{36}$$

where

$$\lambda = \frac{J_e + J_p}{J_e} \tag{37}$$

Although the J-integral solution is difficult to simplify into a reasonable design procedure, some general trends can be observed that will be used to formulate an empirical design expression for λ: J_e is directly proportional to σ^2 (see Equation 32) and J_p is directly proportional to σ^{n+1} (see Equation 34). Equation 38 accounts for these trends and appears to fit the experimental data reviewed in this paper. It is expected that refinements will be made as more data become available.

$$\lambda = 1 + 0.77(\alpha - 1) \tag{38}$$

where

$$\alpha = \frac{\varepsilon}{\varepsilon'_y} \tag{39}$$

DESIGN EQUATION

Derivation of Design Equation

Based on the fracture mechanics equations presented in this paper, a design equation will be derived that accounts for element geometry, constraint and inelastic material behavior. Equation 3 is combined with Equation 4 to get Equation 40.

$$W = 4k_s a u \tag{40}$$

Equation 28 can be expressed as

$$u = F'_y \varepsilon'_y \left(\alpha - \frac{1}{2}\right) \tag{41}$$

And Equation 29 can be expressed as

$$\varepsilon'_y = C_1 \frac{F'_y}{E} \tag{42}$$

where

$$C_1 = 1 - 0.129(C_y + C_z) \tag{43}$$

After substituting the proper values for C_y and C_z:
C_1 = 1.00 for uniaxial stress
= 0.871 for constraint in one direction
= 0.742 for constraint in two directions

Equations 23 and 24 can be expressed as

$$F'_y = C_2 F_y \tag{44}$$

where
C_2 = 1.00 for uniaxial stress
= 1.23 for constraint in one direction
= 1.75 for constraint in two directions

Equations 41, 42 and 44 are combined to get Equation 45.

$$u = C_1 C_2^2 \frac{F_y^2}{E}\left(\alpha - \frac{1}{2}\right) \tag{45}$$

Equation 45 is substituted into Equation 40 to get Equation 46.

$$W = 4k_s a C_1 C_2^2 \frac{F_y^2}{E}\left(\alpha - \frac{1}{2}\right) \tag{46}$$

Equation 5 is substituted into Equation 36 to get Equation 47.

$$J = \lambda \frac{K_I^2}{E} \tag{47}$$

W from Equation 46 is set equal to J from Equation 47 to get Equation 48.

$$\lambda K_I^2 = 4k_s a C_1 C_2^2 F_y^2 \left(\alpha - \frac{1}{2}\right) \tag{48}$$

Equation 10 is substituted into Equation 48 to get Equation 49.

$$\lambda\pi\beta^2\sigma^2 = 4k_s C_1 C_2^2 F_y^2 \left(\alpha - \frac{1}{2}\right) \tag{49}$$

Equation 47 was derived for conditions of plane stress; therefore, for perfectly plastic materials, $\sigma = F_y$. Substituting for F_y simplifies Equation 49 to

$$\lambda\pi\beta^2 = 4k_s C_1 C_2^2 \left(\alpha - \frac{1}{2}\right) \tag{50}$$

To simplify the calculation, C_1 and C_2 can be combined into one variable:

$$C = C_1 C_2^2 \tag{51}$$

where

C = 1.00 for uniaxial stress
= 1.32 for constraint in one direction
= 2.27 for constraint in two directions

Equations 50 and 51 are combined to give Equation 52, which is recommended for design.

$$\begin{aligned} \tan\theta &= \frac{1}{k_s} \\ &= \frac{4C\left(\alpha - \frac{1}{2}\right)}{\pi\lambda\beta^2} \end{aligned} \tag{52}$$

General Trends of the Solution

Figure 13 shows the stress dispersion angle, θ, versus normalized strain, α, according to Equation 52. The general trends of the equation will now be discussed in relation to the behavior observed in the tests.

The effect of element geometry is accounted for in Equation 52 with the variable, β. For edge loading, the dispersion angle is reduced by $1/\beta^2 = 0.797$. The dispersion angles suggested by Young and Hancock (2000) show an average reduction of 0.710 for end-loaded members, which is a 12% difference between the test results and the proposed design procedure. Therefore, the general trend of Equation 52 is correct, but the accuracy is difficult to determine with the limited number of test results that are available.

The effect of constraint is accounted for with the variable, C. The effect of constraint can be observed by comparing the gusset plate tests to the web local yielding tests. Gusset plates are plane stress elements. For web local yielding, the element is restrained in two directions. In the existing research discussed in previous sections of this paper, dispersion angles of 22° to 45° were reported for gusset plates and 49° to 74° were reported for web local yielding. Figure 13 shows that the calculated dispersion angle increases with restraint; therefore, the general trend of Equation 52 is correct.

Inelastic material behavior is accounted for directly with α; however, the dispersion angle is also affected by λ, which varies with the level of inelasticity. Here, λ accounts for the difference between elastic fracture mechanics solution and the inelastic solution. Experimental observations of Graham et al. (1959), Aribert et al. (1981), Hendrick and Murray (1983), Yamamoto et al. (1985) and Cheng and Grondin (1999) showed that the stress dispersion angle increases with inelastic material behavior. This behavior is modeled well with Equation 52.

CALIBRATION OF ALPHA

It has been established that Equation 52 properly accounts for the variables affecting the dispersion angle. If the equation is to be used for design purposes, the level of inelasticity that can be tolerated must be established. Some elements must be designed essentially in the elastic range, such as

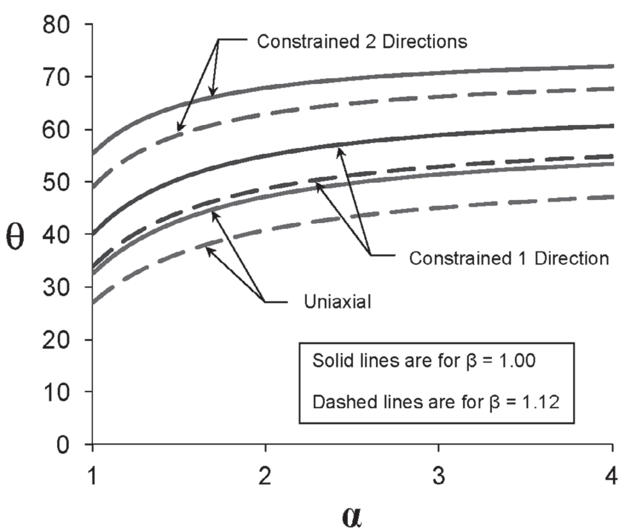

Fig. 13. Stress dispersion angle versus normalized strain.

slender elements susceptible to buckling and elements under high-fatigue cycles. If no inelastic action is expected, $\alpha = 1$. However, most elements in structural steel buildings can be designed under the assumption of at least some inelastic action. The design values for α will be selected to match existing test data reviewed in previous sections of this paper.

To provide reasonable agreement with the experimental results, a value of $\alpha = 1.7$ can be used for elements with adequate ductility to allow some inelastic deformation, but subject to stability problems after yielding. This includes elements such as gusset plates and beam webs. So, $\alpha = 3.8$ can be used for elements with adequate ductility to allow inelastic deformation without the possibility of buckling. This commonly occurs where the load is dispersed through a beam flange and *k*-distance for local web yielding calculations. Here, $\alpha = 10$ can be used for elements with adequate ductility to allow large inelastic deformations without the possibility of buckling. This is recommended for ultimate strength calculations. Table 1 lists the dispersion angles for all combinations with $\beta = 1$ and 1.12; $\alpha = 1.0$, 1.7, 3.8 and 10; and the three conditions of restraint discussed in this paper.

Gusset Plates

The early research on gusset plates focused on elastic stress distribution, and the proposed dispersion angle of 30° has been adopted in design; however, more recent studies by Cheng and Grondin (1999) showed that dispersion angles of 45° can be used if some inelasticity is tolerable. The proposed design procedure using $\beta = 1.00$ and $C = 1.00$ predicts 32.5° for plates with no inelastic capacity and 44.8° for inelastic design with $\alpha = 1.7$.

For conditions wherein the effective width extends beyond the plate boundaries as shown in Figure 14, $\beta = 1.12$ may be appropriate, although the test results are inconclusive for this type of plate geometry. For $C = 1.00$, the dispersion angle is 26.9° for plates with no inelastic capacity and 38.4° for inelastic design with $\alpha = 1.7$.

Web Local Yielding

There is an abundance of test data at various levels of inelasticity to calibrate α for local web yielding calculations, where the stress disperses through the *k*-distance of the beam (θ_1 in Figure 15). For interior loads, $\beta = 1.00$ and the element is constrained by the flange in two directions, which gives calculated values of $\theta = 55.3°$ when $\alpha = 1.0$, $\theta = 71.7°$ when $\alpha = 3.8$, and $\theta = 73.9°$ when $\alpha = 10$.

For elastic load levels, Aribert et al. (1981) proposed a dispersion angle of 49.0°, which is more conservative than the 55.3° angle calculated with Equation 52 at $\alpha = 1.0$.

For design load levels where some inelastic deformation can be accommodated, Sherbourne and Jensen (1957) proposed a 63.4° dispersion angle. Graham et al. (1959) and Aribert et al. (1981) suggested a value of 68.2°, and Hendrick and Murray (1983) recommended 71.6°. All of these empirical dispersion angles fall between the values calculated with $\alpha = 1.0$ and $\alpha = 3.8$; however, the 71.6° angle suggested by Hendrick and Murray (1983) is essentially equal to the calculated value of 71.7° with $\alpha = 3.8$.

At ultimate loads, Graham et al. (1959), and Aribert et al. (1981) proposed a value of 74.0°, which agrees well with the 73.9° angle calculated with $\alpha = 10$.

For conditions wherein the concentrated load is near the end of the member as shown in Figure 16, $\beta = 1.12$ may be appropriate. For $C = 2.27$, the dispersion angle is 49.0° for elements with no inelastic capacity and 67.5° for inelastic design with $\alpha = 3.8$.

Beam Webs

The tests by Young and Hancock (2000) on cold-formed channels reveal some information regarding the dispersion angle through beam webs, shown as θ_2 in Figure 15. Although the value of α is difficult to determine for the experiments, the inelastic capacity is expected to be minimal due to stability problems associated with the thin-walled channels that were tested. At interior loads, they suggested an average dispersion angle of 53.5°, which is much greater than 40.4°, the elastic value for θ calculated with $\beta = 1.00$ and $C = 1.32$ (constrained in one direction). The test results agree better with Equation 52 with $\alpha = 1.7$, which gives $\theta =$ 52.7°.

At end loads, Young and Hancock (2000) suggested an average angle of 38.0°, which falls between the calculated values of 33.8° when $\alpha = 1.0$ and 46.3° when $\alpha = 1.7$. These angles were calculated with $\beta = 1.12$ and $C = 1.32$.

Crane Beams

For the crane beam in Figure 8, the dispersion angle through the rail and top flange can be calculated assuming constraint

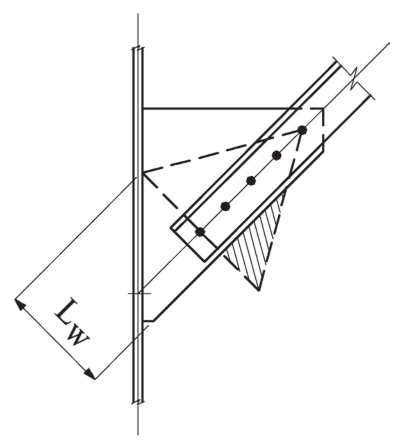

Fig. 14. Effective width beyond the plate boundaries.

Table 1. Dispersion Angles			
β	α	Constraint	θ (degrees)
1.00	1.0	no constraint	32.5
		one direction	40.4
		two directions	55.3
	1.7	no constraint	44.8
		one direction	52.7
		two directions	66.1
	3.8	no constraint	53.1
		one direction	60.4
		two directions	71.7
	10	no constraint	56.8
		one direction	63.6
		two directions	73.9
1.12	1.0	no constraint	26.9
		one direction	33.8
		two directions	49.0
	1.7	no constraint	38.4
		one direction	46.3
		two directions	60.9
	3.8	no constraint	46.7
		one direction	54.5
		two directions	67.5
	10	no constraint	50.6
		one direction	58.1
		two directions	70.1

in two directions with $\beta = 1.00$, which gives $\theta = 55.3°$ for $\alpha = 1.00$. This is less than the value of 60° suggested by Ricker (1982), but shows that the value of 45° adopted in CMAA (1994), AS (2001) and AISE (1997) is overly conservative.

Welded Plate

For connections with a plate welded to the flange of a member as shown in Figure 17, the flange can be considered constrained in two directions, and the effective width of the plate can be calculated with a dispersion angle of 55.3° for plates with no inelastic capacity and 71.7° for inelastic design with $\alpha = 3.8$.

PROPOSED DESIGN PROCEDURE

An appropriate design value for the stress dispersion angle, θ, can be calculated with the following design procedure:

- Select an appropriate value for α based on the inelastic capacity (see Table 2).
- Calculate λ with Equation 38.

$$\lambda = 1 + 0.77(\alpha - 1) \tag{38}$$

- Determine the constraint factor, C.
  C = 1.00 for uniaxial stress
  = 1.32 for constraint in one direction
  = 2.27 for constraint in two directions
- Determine the geometry factor, β.
  Under normal conditions, $\beta = 1.00$
  If the effective width extends beyond the edge of the element as shown in Figures 14 and 16, $\beta = 1.12$

Table 2. Design Values for α		
α	**Inelastic Capacity**	**Examples**
1.0	essentially elastic	slender elements elements with high fatigue cycles
1.7	some inelastic deformation with potential for inelastic buckling	gusset plates beam webs
3.8	some inelastic deformation—no buckling	local web yielding
10	large inelastic deformation—no buckling	ultimate strength calculations

- Calculate θ with Equation 52.

$$= \frac{4C\left(\alpha - \frac{1}{2}\right)}{\pi\lambda\beta^2} \qquad (52)$$

CONCLUSIONS

The existing literature contains a wide range of recommended dispersion angles for stress flow around discontinuities in steel structures. Therefore, it is important to determine the variables affecting the stress flow so that the proper dispersion angles can be used in design.

Using fracture mechanics, it was shown that the dispersion angle is dependent on geometry, constraint and inelastic deformation capacity. An analytical model was derived that accounts for all variables affecting the dispersion angle. The model was shown to properly predict the experimental trends. A versatile design procedure, which explicitly accounts for all variables affecting the stress dissipation angle, was presented. Because the design variables related to the inelastic capacity were calibrated to the test results, the proposed design values agree well with the experimental values.

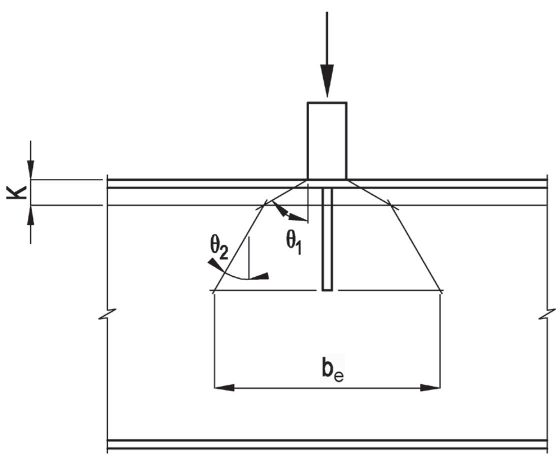

Fig. 15. Effective width of a beam web subjected to a concentrated load.

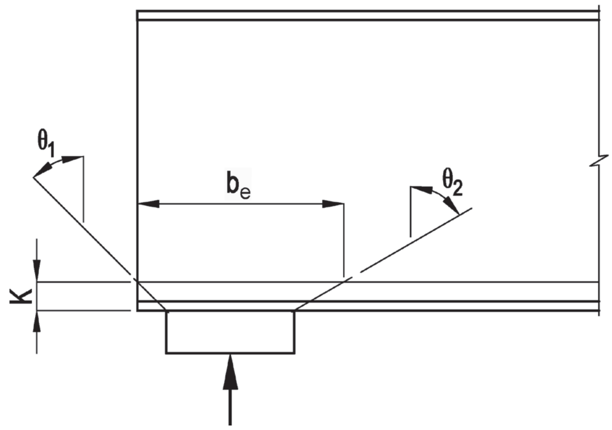

Fig. 16. Effective width of a beam web subjected to a concentrated end load.

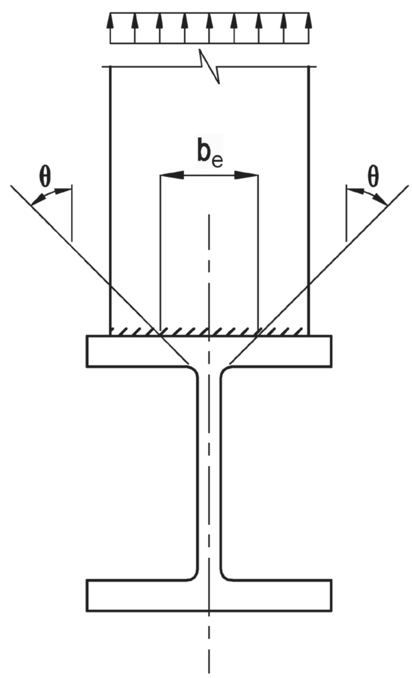

Fig. 17. Effective width of a plate welded to a column flange.

REFERENCES

Abi-Saad, G. and Bauer, D. (2006), "Analytical Approach for Shear Lag in Welded Tension Members," *Canadian Journal of Civil Engineering*, Vol. 33, pp. 384–394.

ABS (2009), *Common Structural Rules for Double Hull Oil Tankers*, American Bureau of Shipping, July.

AISC (1937), *Specification for the Design, Fabrication and Erection of Structural Steel for Buildings*, American Institute of Steel Construction, New York, NY.

AISC (2010), *Specification for Structural Steel Buildings*, June 22, American Institute of Steel Construction, Chicago, IL.

AISC (2011), *Steel Construction Manual*, 14th ed., American Institute of Steel Construction, Chicago, IL.

AISE (1997), *Guide for the Design and Construction of Mill Buildings*, AISE Technical Report No. 13, Association of Iron and Steel Engineers.

Aribert, J.M., Lauchal, A. and Nawawy, O.I. (1981), "Elastic-Plastic Modelization of the Resistance of a Column Web in the Compression Region," *Construction Métallique*, No. 2, June.

AS (2001), *Cranes, Hoists and Winches, Part 18: Crane Runways and Monorails*, Australian Standard, AS 1418.18.

ASME (2001), *Steel Stacks*, ASME STS-1-2000, American Society of Mechanical Engineers.

Bažant, Z.P. and Cedolin, L. (1991), *Stability of Structures, Elastic, Inelastic, Fracture, and Damage Theories*, Oxford University Press, New York, NY.

Bjorhovde, R. and Chakrabarti, S.K. (1985), "Tests of Full-size Gusset Plate Connections," *Journal of Structural Engineering,* ASCE, Vol. 111, No. 3, pp. 667–683.

Blodgett, O.W. (1998), "The Effect of Constraint on Ductility in Welded Beam-to-Column Connections," Seminar notes from the seminar, *Design of Welded Structures,* by the Lincoln Electric Company.

Boresi, A.P., Schmidt, R.J. and Sidebottom, O.M. (1993), *Advanced Mechanics of Materials*, 5th ed., John Wiley and Sons, New York, NY.

Broek, D. (1986), *Elementary Engineering Fracture Mechanics*, 4th ed., Kluwer Academic Publishers.

Chakrabarti, S.K. (1983), *Tests of Gusset Plate Connections,* M.S. Thesis, University of Arizona, Tucson, AZ.

Chen, W.F. and Han, D. (1988), *Plasticity for Structural Engineers*, Springer-Verlag, New York, NY.

Cheng, J.J.R. and Grondin, G.Y. (1999), "Recent Development in the Behavior of Cyclically Loaded Gusset Plate Connections," *Proceedings, North America Steel Construction Conference*. American Institute of Steel Construction, Chicago, IL, pp. 8-1 – 8-22.

Chesson, E. and Munse, W.H. (1963), "Riveted and Bolted Joints: Truss-Type Tensile Connections," *Journal of the Structural Division, Proceedings of the American Society of Civil Engineers,* Vol. 89, No. ST1, February, pp. 67–106.

CICIND (1999), *Model Code for Steel Chimneys*, Revision 1, Hertfordshire, UK.

CMAA (1994), *Specifications for Top Running Bridge and Gantry Type Multiple Girder Electric Overhead Traveling Cranes*, Specification 70, Crane Manufacturers Association of America.

Cook, R.D. and Young, W.C. (1985), *Advanced Mechanics of Materials*, Macmillan Publishing Company, New York, NY.

Eurocode (2005), Eurocode 3: Design of Steel Structures—Part 1-8: Design of Joints, European Standard, EN 1993-1-8.

Girard, C., Picard, A. and Fafard, M. (1995), "Finite Element Modeling of the Shear Lag Effects in an HSS Welded to a Gusset Plate," *Canadian Journal of Civil Engineering,* Vol. 22, pp. 651–659.

Gould, P.L., Sen, S.K., Wang, R.S.C., Suryoutomo, H. and Lowery, R.D. (1976), "Column Supported Cylindrical-Conical Tanks," *Journal of the Structural Division*, Vol. 102, No. ST2, February, pp. 429–447.

Graham, J.D., Sherbourne, A.N., Khabbaz, R.N. and Jensen, C.D. (1959), *Welded Interior Beam-to-Column Connections*, American Institute of Steel Construction, Chicago, IL.

Griffith, A.A. (1920), "The Phenomena of Rupture and Flow in Solids," *Philosophical Transactions of the Royal Society of London*, Series A, Vol. 221, pp. 163–198.

Gross, J.L. and Cheok, G. (1988), *Experimental Study of Gusseted Connections for Laterally Braced Steel Buildings,* National Institute of Standards and Technology, Gaithersburg, MD, November.

He, M.Y. and Hutchinson, J.W. (1983), "Fully-Plastic J-Solutions for Cracks in Infinite Solids," *Elastic-Plastic Fracture, Second Symposium,* Vol. 1, ASTM STP 803, American Society for Testing and Materials.

Hendrick, A. and Murray, T.M. (1983), "Column Web and Flange Strength at End-Plate Connections," Report FSEL/AISC 83-01, School of Civil Engineering and Environmental Science, University of Oklahoma.

Irvan, W.G. (1957), "Experimental Study of Primary Stresses in Gusset Plates of a Double Plane Pratt Truss," University of Kentucky Engineering Research Station Bulletin No. 46, December.

Irwin, G.R. (1957), “Analyses of Stresses and Strains Near the End of a Crack Traversing a Plate,” *Journal of Applied Mechanics*, ASME, Vol. 24, pp. 361–364.

Kaups, T. and Lieb, J.M., (1986), “A Practical Guide for the Design of Quality Bulk Storage Bins and Silos,” *International Journal of Bulk Solids Storage in Silos*, Vol. 2, No. 2, pp. 9–24.

Kumar, V., German, M.D. and Shih, C.F. (1981), “An Engineering Approach for Elastic-Plastic Fracture Analysis,” EPRI Report NP-1931, Electric Power Research Institute, Palo Alto, CA, July.

Lavis, C.S. (1967), *Computer Analysis of the Stresses in a Gusset Plate*, Master’s Thesis, University of Washington, Seattle, WA.

Murray, T.M. and Sumner, E.A. (2003), *Extended End-Plate Moment Connections, Seismic and Wind Applications*, Steel Design Guide 4, 2nd ed., American Institute of Steel Construction, Chicago, IL.

NIST (2005), *Mechanical Properties of Structural Steels*, Federal Building and Fire Safety Investigation of the World Trade Center Disaster, U.S. Department of Commerce, September.

Owens, G.W. and Cheal, B.D. (1989), *Structural Steelwork Connections*, Butterworths, London, UK.

Pasternak, H. (2002), “Silos and Tanks,” *Refurbishment of Buildings and Bridges*, CISM Course 435, Chapter 3, edited by Mazzolani, F.M. and Ivanyi, M., Springer, pp. 166–180.

Rabern, D.A. (1983), *Stress, Strain and Force Distributions in Gusset Plate Connections*, Master’s Thesis, University of Arizona, Tucson, AZ.

Ramberg, W. and Osgood, W.R. (1943), “Description of Stress-Strain Curves by Three Parameters,” Technical Note 902, National Advisory Committee for Aeronautics, July.

Rice, J.R. (1968), “A Path-Independent Integral and the Approximate Analysis of Strain Concentration by Notches and Cracks,” *Journal of Applied Mechanics*, ASME, Vol. 35, pp. 379–386.

Ricker, D.T. (1982), “Tips for Avoiding Crane Runway Problems,” *Engineering Journal*, American Institute of Steel Construction, Vol. 19, No. 4, Fourth Quarter.

Sandel, J.A. (1950), *Photoelastic Analysis of Gusset Plates*, Master’s Thesis, University of Tennessee, Knoxville, TN, December.

Sherbourne, A.N. and Jensen, C.D. (1957), *Direct Welded Beam Column Connections*, Report No. 233.12, Fritz Laboratory, Lehigh University, Bethlehem, PA.

Shih, C.F. and Hutchinson, J.W. (1976), “Fully Plastic Solutions and Large-Scale Yielding Estimates for Plane Stress Crack Problems,” *Journal of Engineering Materials and Technology*, Vol. 98, pp. 289–295.

Smith, E. and Pilkington, R. (1978), “The Characterization of Crack-Tip Deformation Fields in Non-Linear Materials,” *Non-Linear Problems in Stress Analysis*, P. Stanley, ed., Applied Science Publishers.

Wang, S. (1974), *Design of Cylindrical Steel Tanks Subjected to Concentrated Support Loads*, Ph.D. Dissertation, Washington University, St. Louis, MO, December.

Whitmore, R.E. (1952), “Experimental Investigation of Stresses in Gusset Plates,” University of Tennessee Engineering Experiment Station Bulletin No. 16, May.

Wolf, C.D. (1983), “Structural Design Aspects of Materials Handling Plant,” *Metal Structures Conference*, *Proceedings,* Brisbane, Australia, The Institution of Engineers, May, pp. 148–158.

Wozniak, R.S. (1990), “Steel Tanks,” *Structural Engineering Handbook*, 3rd ed., Section 27, E.H. Gaylord and C.N. Gaylord, eds., McGraw-Hill, New York, NY.

Wyss, T. (1923), “Die Kraftfelder in Festen Elastischen Korpern und ihre Praktischen Anwendungen,” Berlin, Germany (in German).

Yamamoto, K., Akiyama, N. and Okumara, T. (1985), “Elastic Analysis of Gusseted Truss Joints,” *Journal of Structural Engineering,* ASCE, Vol. 111, No. 12, December, pp. 2545–2564.

Young, B. and Hancock, G.J. (2000), “Tests and Design of Cold-Formed Unlipped Channels Subjected to Web Crippling,” *Proceedings of the Fifteenth International Specialty Conference on Cold-Formed Steel Structures*, St. Louis, MO, October 19–20, pp. 43–70.

Zhao, Y. and Yu, J. (2005), “Stability Behavior of Column-Supported Steel Silos with Engaged Columns,” *Advances in Steel Structures*, *Proceedings of the Fourth International Conference,* edited by Shen, Z.Y., Li, G.Q. and Chan, S.L., June.

Overview of the Development of Design Recommendations for Eccentrically Braced Frame Links with Built-Up Box Sections

JEFFREY W. BERMAN and MICHEL BRUNEAU

ABSTRACT

Among the new additions to the 2010 AISC *Seismic Provisions* are design requirements for eccentrically braced frame links with built-up box sections. Such links do not require lateral bracing in many cases because built-up box shapes have superior lateral torsional stability relative to wide flange sections. The 2010 *Seismic Provisions* include requirements for built-up box link flange width-to-thickness ratio and other important design considerations. However, the limits on web width-to-thickness ratio default to those used for built-up box beams or columns and are inadequate for links with large inelastic shear and compression strains. Such limits are important for preventing web buckling under shear and/or flexural compression. This paper presents an overview of research on the design and behavior of links with built-up box sections, including the development of recommendations for web width-to-thickness limits and corresponding web stiffener spacing requirements and flange width-to-thickness limits for these link sections. The highlighted research program included derivation of design requirements based on plate buckling considerations; a full-scale, single-story eccentrically braced frame test; a parametric study on the impact of link cross-sectional parameters on link inelastic rotation capacity; and a series of large-scale tests on isolated links.

Keywords: eccentrically braced frames, built-up box sections, links, width-to-thickness limits.

INTRODUCTION

New design requirements for eccentrically braced frame (EBF) links with built-up box sections now appear in the 2010 AISC *Seismic Provisions* (AISC, 2010). Prior to this edition, the *Seismic Provisions* only addressed design and detailing requirements for links with I-shaped cross-sections. Built-up box links may be desirable for a number of practical situations because they have much a larger resistance to lateral torsional buckling than I-shaped links. In many cases, this eliminates the need for link lateral bracing beyond that provided by the eccentric braces. For example, when EBFs are used in elevator cores or stairwells, it may be difficult to laterally brace I-shaped links as required to prevent lateral buckling, whereas built-up box sections may be used without the need for additional lateral bracing.

The 2010 *Seismic Provisions* address most of the design and detailing considerations for EBFs with built-up box links, including the design link shear strength, link stiffener requirements, and welding requirements. However, the flange width-to-thickness requirements and web width-to-thickness requirements for built-up box links are, by default, those for built-up box shapes used as beams or columns in Table D1.1 of the 2010 AISC *Seismic Provisions,* and Section F3.5b requires that the limits for highly ductile members be used. For links in EBFs, the compressive strains in the flanges are generally lower than those for moment frames, and flange buckling is less of a concern, especially for short links. Limits on the web width-to-thickness ratio for built-up box links are important to inhibit web buckling prior to achieving the required inelastic link rotation level. As discussed later, the webs of built-up box links may be subjected to large shear stresses when the links are short and the behavior is dominated by shear yielding. In these cases, web stiffeners are effective for inhibiting web buckling when the web width-to-thickness is large. When links are longer and the inelastic flexural behavior plays a more important role, the webs may have large flexural compression stresses, and web stiffeners are ineffective in preventing web buckling. Thus, to inhibit web buckling and ensure the links can achieve the desired ductility, it is necessary to have web width-to-thickness ratio limits that address these different conditions. Bruneau (2013) provides recommended web width-to-thickness ratio limits that are a result of the research briefly reviewed here.

To develop the design recommendations for links with built-up box sections, a study was conducted that included derivation of local buckling prevention requirements from plate buckling considerations and development of link plastic strength equations; a large-scale experiment on a single-story EBF with a built-up box section; parametric finite

Jeffrey W. Berman, Ph.D., Associate Professor, Department of Civil and Environmental Engineering, University of Washington, Seattle, WA. E-mail: jwberman@uw.edu

Michel Bruneau, P.Eng., Professor, Department of Civil and Environmental Engineering, University at Buffalo, Buffalo, NY (corresponding author). E-mail: bruneau@buffalo.edu

element analyses of links with various sections; and large-scale testing of isolated links to evaluate the final design recommendations. A brief overview of these studies is provided here. Emphasis is placed on the development of recommendations for link width-to-thickness limits and web stiffener requirements—the key issues pertinent to designers who may wish to use links with built-up box sections.

LINK DESIGN EQUATIONS

Link Strength

Figure 1 shows a schematic of an EBF link with length, e, and a built-up box cross-section that consists of four plates welded together with external (Figure 1b) or internal (Figure 1c) stiffeners at a spacing, a. For links with doubly symmetric cross-sections of this type, the plastic flexural capacity, M_p, is given by

$$M_p = F_{yf} t_f \left(b_f - 2t_w\right)\left(d - t_f\right) + F_{yw} \frac{t_w d^2}{2} \tag{1}$$

where t_w is the web thickness, t_f is the flange thickness, d is the section depth, b_f is the section width, F_{yf} is the yield strength of the flange plate material and F_{yw} is the yield strength of the web plate material. Figure 1 also identifies the free flange width, b, and the free web depth, h. The plastic shear strength, V_p, is

$$V_p = \frac{2}{\sqrt{3}} F_{yw} t_w \left(d - 2t_f\right) \tag{2}$$

Similar to links with wide flange sections, the link length, e, plastic moment strength and plastic shear strength can be used to determine whether links will yield predominantly in shear, flexure or a mix of both. Links with $e \leq 1.6\ (M_p/V_p)$ will yield primarily in shear and are denoted "shear links"; links with $e \geq 2.6\ (M_p/V_p)$ will yield primarily in flexure and are denoted "flexural links"; links with lengths between those bounds will yield in a combination of shear and flexure and are denoted "intermediate links." Note that Berman and Bruneau (2005) derived expressions for shear and flexural strength that accounted for shear-flexural interaction. However, test results reported in Berman and Bruneau (2006) showed that even intermediate links were able to simultaneously achieve both their plastic shear and flexural strengths due to strain hardening. Similar observations were made for I-shaped links by Roeder and Popov (1978) and Kasai and Popov (1986). Thus, the *Seismic Provisions* neglect shear-flexural interaction for links of all lengths and cross-sections.

Link Flange Width-to-Thickness Ratio

To achieve ductile link behavior, it is necessary to delay the onset of flange local buckling until significant inelastic rotation has been achieved. Flange local buckling can cause strength degradation, precipitate flange fracture and also trigger web or lateral torsional buckling. Limiting flange width-to-thickness ratios (b_f/t_f) were derived by Kasai and Popov (1986) for EBF links with I-shaped cross-sections, and a similar derivation is used with necessary modifications

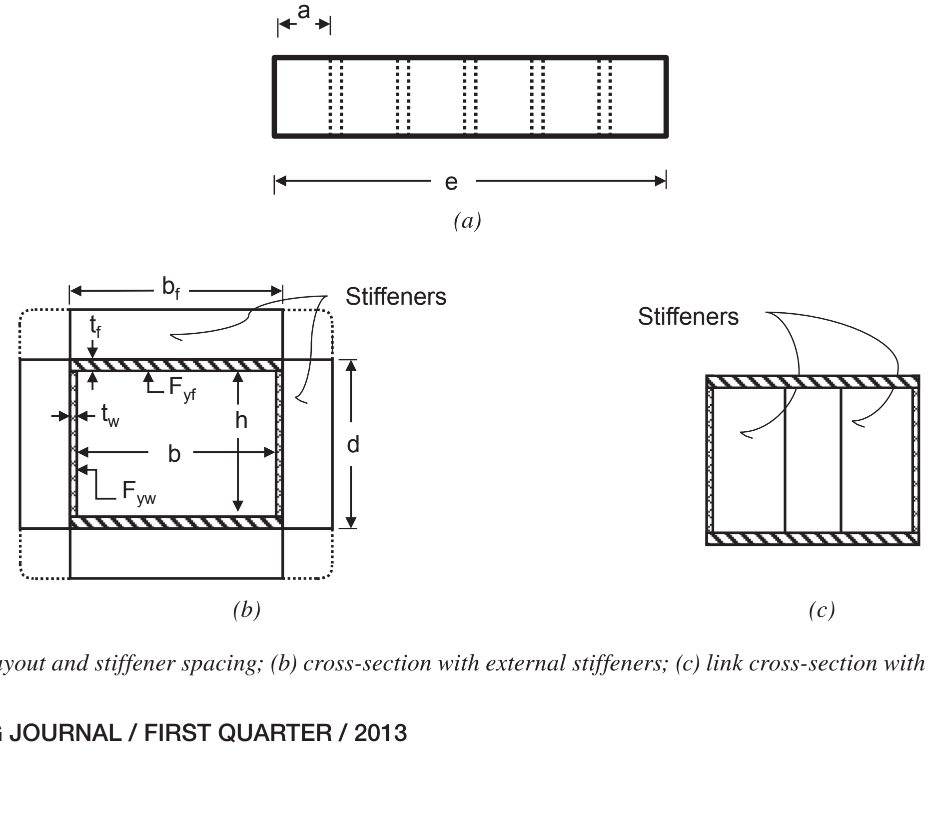

Fig. 1. (a) Link layout and stiffener spacing; (b) cross-section with external stiffeners; (c) link cross-section with internal stiffeners.

specific to built-up box sections. First the flange yield length is determined, which is the length of flange from the link end expected to yield; then the maximum flexural or shear strength of the link is achieved. This value is then introduced in a plastic plate buckling equation to determine the critical buckling stress of the flange element, which in turn is compared with an estimate of the average flange stress in the flange yield zone.

To determine the flange yield length for a general case of unequal link end moments and the presence of an axial load, Kasai and Popov (1986) used the link free-body diagram and moment diagram shown in Figure 2, where M_A and M_B are the end moments at the right and left ends, respectively, with M_A being greater than or equal to M_B and also greater than the plastic moment capacity of the link M_p because of strain hardening; V is the link shear force; α is the ratio of link axial force to link shear force; e_i is the distance from the right link end to the inflection point; l_y is the flange yield length; and γ is the link rotation angle. Using the free-body diagram of Figure 2, the plastic moment capacity of the link accounting for a reduction due to axial load but neglecting any reduction due to shear, M_{pa}, can be written as

$$M_{pa} = \left(F_y - \frac{\alpha V}{A_g}\right) Z_x = \left(F_y - \frac{\alpha M_A}{e_i A_g}\right) Z_x = \left(1 - \frac{\alpha M_A}{e_i P_Y}\right) M_p \quad (3)$$

Additionally, using the moment diagram of Figure 2, the reduced plastic moment accounting for a reduction due to axial load may be written as

$$M_{pa} = M_A \left(1 - \frac{l_y}{e_i}\right) \quad (4)$$

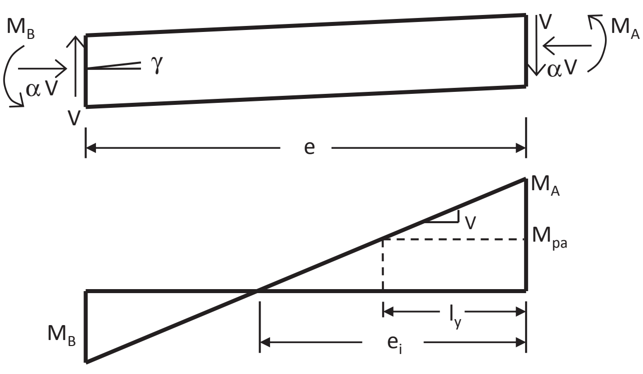

Fig. 2. Link free-body diagram and moment diagram (adapted from Kasai and Popov, 1986).

Setting Equations 3 and 4 equal and solving for the flange yield length gives

$$l_y = e_i \left(1 - \frac{M_p}{M_A}\right) + \frac{\alpha M_p}{P_y} \quad (5)$$

Within the flange yield zone, the average stress is the average of F_{yf} and the flange stress corresponding to moment M_A. To match strain gauge data from tests on links with wide flange sections, Kasai and Popov (1986) modified the average flange stress to be

$$\sigma_{av} = \frac{F_{yf}}{2} \left(1 + \frac{1.1 M_A}{M_p}\right) \quad (6)$$

The inelastic plate buckling stress for boundary conditions consistent with that of the flange of a built-up box section—namely, with all edges supported against vertical translation but unrestrained against rotation—was derived by Haaijer (1957) as

$$\sigma_b = \frac{\pi^2}{12} \left(\frac{t_f}{b}\right)^2 \left[D_x \left(\frac{b}{l_h}\right)^2 + D_y \left(\frac{l_h}{b}\right)^2 + D_{xy} + D_{yx} + 4G_t \right] \quad (7)$$

where D_x, D_y, D_{xy} and D_{yx} are plastic plate modulii in the longitudinal (x), transverse (y) and shear (xy and yx) directions; G_t is the plastic shear modulus; l_h is the half wavelength of the buckled plate; and b is the free width of the flange. Based on numerous compression tests, Haaijer determined the following values to be appropriate for this moduli: D_x = 3,000 ksi; D_y = 32,800 ksi; $D_{xy} = D_{yx}$ = 8,100 ksi; G_t = 2,400 ksi. Equation 7 can be used to calculate the plastic flange buckling stress of links with built-up box cross-sections, with the half-wavelength taken as the smaller of the stiffener spacing, or $l_y/2$, where l_y is given by Equation 5. The average flange stress can then be compared with the inelastic plate buckling stress to determine if the flange is likely to buckle.

For shear links, several simplifications and assumptions may be made to reduce the preceding equations to a width-to-thickness limit. First, Haaijer (1957) showed that the minimum plastic buckling stress occurs when

$$\frac{l_h}{b} = 4\sqrt{\frac{D_x}{D_y}} \quad (8)$$

which for the values provided earlier gives $l_h = 0.55 b_f$. Using this in Equation 7 gives the minimum plastic buckling stress.

The maximum average flange stress may be found by estimating the maximum end moment, M_A, for a shear link to be

$$M_A = 1.35\,V_p\,\frac{e}{2} \tag{9}$$

where e is the total link length and 35% strain hardening is assumed as a reasonable upper bound. The theoretical maximum link length, e^*, for a shear link is

$$e^* = \frac{2M_p}{V_p} \tag{10}$$

Using Equations 9 and 10 in Equation 6 gives the average flange stress in the flange yield zone to be

$$\sigma_{av} = 1.243F_{yf} \tag{11}$$

Limiting the average flange stress in Equation 11 to the plastic buckling stress in Equation 7 and inserting Equation 8 for the half-buckling wavelength, along with the given values for the plastic plate moduli, gives an estimate of the b/t_f for shear links to prevent flange buckling

$$\frac{b}{t_f} \le \frac{174}{\sqrt{F_{yf}}} = 1.02\sqrt{\frac{E}{F_{yf}}} \tag{12}$$

where E is the modulus of elasticity. For flexural links, M_A may be approximated by $1.2M_p$, resulting in an average flange stress of $1.292F_{yf}$ in the flange yield zone and a limiting width-to-thickness ratio of

$$\frac{b}{t_f} \le \frac{170}{\sqrt{F_{yf}}} = 1.00\sqrt{\frac{E}{F_{yf}}} \tag{13}$$

Note that this is different from the b/t_f limit for hollow rectangular sections in the 2010 AISC *Seismic Provisions,* which are

$$\frac{b}{t_f} \le 0.64\sqrt{\frac{E}{F_{yf}}} \quad \text{for moderately ductile members} \tag{14a}$$

$$\frac{b}{t_f} \le 0.55\sqrt{\frac{E}{F_{yf}}} \quad \text{for highly ductile members} \tag{14b}$$

which is the result of work by Lee and Goel (1987) and Hassan and Goel (1991) on fracture and local buckling prevention in concentrically braced frames, based on test results using hollow structural section (HSS) braces. However, the derivation and limits in Equations 12 and 13 do not account for accumulated plastic strain due to cyclic loading. As discussed in the following section, finite element analyses demonstrated that, in many cases, the more restrictive limit of Equation 14a for moderately ductile members was necessary to limit flange local buckling in built-up box links when several cycles of inelastic behavior are considered.

Stiffener Spacing and Web Buckling

Web buckling has also been shown to be an undesirable failure mode for links in EBFs because it causes rapid strength and stiffness degradation. In shear links, the webs are under primarily shear stress, and prevention of web buckling can be achieved through the use of vertical web stiffeners. For shear links of any section, the required stiffener spacing to limit web buckling up to a desired link rotation is a critical design issue. Kasai and Popov (1986) derived the stiffener spacing formula for links with I-shaped sections that appears in the AISC *Seismic Provisions*. The following derivation of a stiffener spacing formula for links with built-up box sections is similar to that for links with I-shaped sections, modified to represent the appropriate web boundary conditions. Note that web width-to-thickness ratio (h/t_w) limits are not directly derived here but are instead based on observations from experiments and finite element analyses as described later.

Kasai and Popov (1986) showed that the required stiffener spacing for shear links could be found by considering the inelastic shear buckling stress, τ_b, given by

$$\tau_b = \eta(\gamma)\tau_E \tag{15}$$

where $\eta(\gamma)$ is a plastic reduction factor and is a function of the strain history, and τ_E is the elastic shear buckling stress for a plate given by

$$\tau_E = \frac{\pi^2 E}{12\left(1-\upsilon^2\right)} K_s(\alpha)\left(\frac{1}{\beta}\right)^2 \tag{16}$$

where υ is Poisson's ratio; $K_s(\alpha)$ is a buckling coefficient, which is a function of the boundary conditions; and the panel aspect ratio, α, itself is defined as the stiffener spacing, a, over the web depth, $h = d - 2t_f$. Also, β is the web width-to-thickness ratio defined as the web depth over the web thickness, t_w (Basler, 1961).

Kasai and Popov used tests of links with wide flange sections having various yield strengths, aspect ratios, web width-to-thickness ratios and load histories to relate the plastic reduction factor to the secant shear modulus, G_s, and the elastic shear modulus, G, as

$$\eta = 3.7\frac{G_s}{G} \tag{17}$$

The secant shear modulus is

$$G_s = \frac{\tau_b}{\overline{\gamma}_b} \tag{18}$$

where τ_b is the shear stress at web buckling (the shear force at web buckling divided by the web area), $\overline{\gamma}_b$ is the link rotation from the last point of zero shear force in the load history to the onset of web buckling, and the elastic shear modulus is

$$G = \frac{E}{2(1-\upsilon)} \tag{19}$$

Substituting Equations 16 through 19 into Equation 15, conservatively approximating $\overline{\gamma}_b$ with $2\gamma_u$, where γ_u is the ultimate link rotation, and solving for γ_u gives

$$\gamma_u = 4.35 K_s(\alpha)\left(\frac{1}{\beta}\right)^2 \tag{20}$$

The boundary conditions for the web of a built-up box section may be approximated by assuming the web is hinged along all four sides. This differs from that used for wide flange cross-sections, where it was assumed that the flange provides the web with restraint against rotation. For a shear buckling of a plate with four sides hinged, Galambos (1998) gives $K_s(\alpha)$ as

$$K_s(\alpha) = 5.34 + \frac{4}{\alpha^2} \quad \text{if} \quad \alpha \ge 1 \tag{21a}$$

$$K_s(\alpha) = 4 + \frac{5.34}{\alpha^2} \quad \text{if} \quad \alpha < 1a \tag{21b}$$

Setting the maximum panel aspect ratio α equal to 1, substituting the appropriate expression for $K_s(\alpha)$ into Equation 20 and solving for α gives

$$\alpha = \sqrt{\frac{5.34}{\left(\frac{\gamma_u \beta^2}{4.35}\right) - 4}} \tag{22}$$

Note that for panel aspect ratios greater than 1, the constants 5.34 and 4 in Equation 22 switch places. Solving Equation 22 for the stiffener spacing, a, can be conservatively approximated by the following, as discussed in Berman and Bruneau (2005):

$$a = C_B t_w - \frac{h}{8} \tag{23}$$

where C_B is 20 for ultimate link rotations of 0.08 rad and 37 for ultimate link rotations of 0.02 rad. Linear interpolation may be used for other link rotation angles. For I-shaped links, C_B is 30 and 52 for the same ultimate link rotations, respectively. Shear links with built-up box sections having stiffener spacing satisfying Equation 23 should not exhibit web buckling prior to reaching the corresponding ultimate link rotation angle. However, as described later, an upper limit on web-to-thickness ratio is necessary even in the presence of stiffeners. Additionally, for links with large flexural compression stresses in the web, stiffeners alone will likely not prevent web buckling, and a more strict web width-to-thickness ratio limit may be necessary.

EXPERIMENTAL AND ANALYTICAL RESEARCH

This section provides an overview of the research program used to investigate the behavior and ductility of links with built-up box sections and to finalize design recommendations. More detailed discussions of the key components of the research program are available in Berman and Bruneau (2007, 2008a and 2008b). The focus here is to concisely indicate the methods used to finalize the design recommendation for links of this type with an emphasis on the limits for flange width-to-thickness ratio, web width-to-thickness ratio, and stiffener spacing and lateral bracing requirements.

Large-Scale, Single-Story EBF with Built-Up Box Link Test

To investigate the lateral stability and ductility of an EBF with a built-up box link, a large-scale, single-story EBF was tested under quasi-static loading at the University at Buffalo. The test setup and link details are shown in Figure 3. The frame was loaded via a loading beam, and lateral restraint was applied only to the loading beam, thus effectively bracing the columns at the story height against out-of-plane movement. Lateral bracing was not applied to the link, to the beam outside the link, to the braces or along the interstory column height. The link was designed to be a shear link; using yield strengths obtained from coupon tests for the web and flange steels, the corresponding calculated plastic shear and moment strengths were 111.3 kips and 116.2 kip-ft, respectively, resulting in an $e/(M_p/V_p)$ ratio of 1.43, thus ensuring that the link would behave as a shear link.

Figure 4 shows the experimental results in terms of base shear force versus story drift and link shear force versus link rotation angle. As shown, the link achieved a maximum total link rotation angle of 0.123 rad, which corresponds to an inelastic rotation angle of 0.11 rad for multiple cycles, and achieved a half cycle at a total rotation angle of 0.151 rad. The target plastic rotation angle for the link was the maximum allowed by the AISC *Seismic Provisions* of 0.08 rad, demonstrating that the link had adequate ductility. There was significant link overstrength, as the peak link shear force was 1.5 times the plastic shear force calculated using the material test results. At an inelastic link rotation angle of 0.08 rad, the link shear was 1.39 times the calculated link plastic shear strength. The maximum link moment exceeded the link plastic moment by 8% at the maximum link rotation, further confirming that, in practice, flexure-shear interaction may be neglected due to strain hardening. No evidence of lateral instability was observed, and the maximum out-of-plane moments in the brace members and beam outside the link were, for the most part, less than 2.5% of the link's plastic moment capacity (Berman and Bruneau, 2005). This test demonstrated that EBFs with built-up box sections can develop adequate ductile response without lateral bracing of the link ends.

Note that the 2010 AISC *Seismic Provisions* specify a limit on the ratio of the strong axis to weak axis link moments of inertias, I_x/I_y, to prevent the use of built-up box links with sections that are significantly more susceptible to lateral instability (as well as to ensure sufficient link stiffness out-of-plane of the frame to laterally restrain the braces

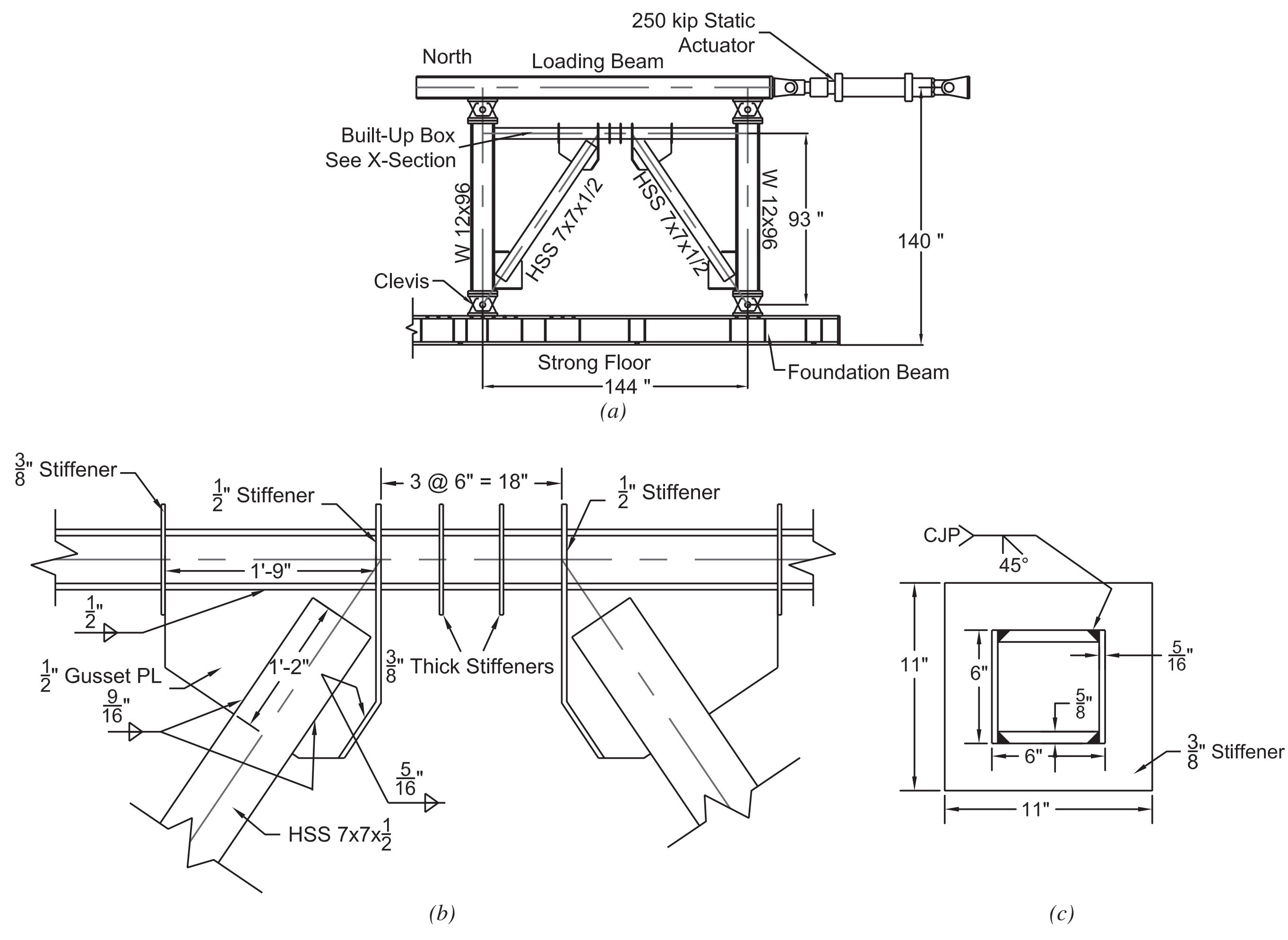

Fig. 3. (a) Large-scale EBF with built-up box link test setup; (b) brace-to-beam connection and link details; (c) link cross-section at stiffeners (adapted from Berman and Bruneau, 2005).

of the eccentrically braced frame). However, it is difficult to achieve links that satisfy the web h/t_w limits discussed later while also having large I_x/I_y. Therefore, in most practical cases, the I_x/I_y, limit is a redundant requirement, and sufficient lateral stability to eliminate the need for lateral bracing of built-up box sections is ensured by simply satisfying the width-to-thickness requirements.

Link Testing and Finite Element Modeling

The b/t_f limits and web stiffener spacing requirements derived earlier do not consider the impact of cyclic inelastic loading. Furthermore, the effect of flexural compression in the webs of intermediate and flexural links necessitates that an upper limit on the web width-to-thickness ratio be used in those cases. To investigate these issues and determine whether the derived requirements are adequate, a series of link finite element analyses and link tests were conducted. A brief overview is provided here, and additional detail can be found in Berman and Bruneau (2008a and 2008b).

The finite element parametric study was conducted in two parts. Part A explored the behavior of links of various cross-sectional dimensions with and without stiffeners and established limits for b/t_f and h/t_w, but used a single material behavior and yield stress. Part B explored the behavior of links with b/t_f and h/t_w at the proposed limits resulting from part A, but with various web and flange yield stresses. All links were modeled using shell elements, and the analyses included material and geometric nonlinearities. The modeling methodology was validated via comparison with the experimental results for the single-story EBF test described briefly earlier and the individual link tests described later.

Each model was subjected to the EBF loading protocol in the 2002 AISC *Seismic Provisions* (AISC, 2002), which specified three cycles at each total link rotation level of 0.0025, 0.005 and 0.01 rad, followed by two cycles at 0.01-rad increments beyond that. That protocol has been demonstrated to be more demanding than the current loading protocol in the 2005 and 2010 AISC *Seismic Provisions* that is based on work by Richards and Uang (2006) and thus should provide conservative results for the plastic rotation capacity of the various links studied. Boundary conditions were applied such that the rotation was restrained at each link end, a vertical displacement was applied at one end of the link corresponding to the target link rotation times the link length, and horizontal translation at the left end was free to prevent the development of link axial force at large rotations. The plastic rotation capacity was taken as the plastic rotation at which the link shear strength had degraded to 80% of the peak strength.

In part A of the finite element parametric study, finite element models were generated for links with lengths of $1.2M_p/V_p$, $1.6M_p/V_p$, $2.1M_p/V_p$ and $3.0M_p/V_p$, having b/t_f values of $0.33\sqrt{E/F_{yf}}$, $0.71\sqrt{E/F_{yf}}$, $1.00\sqrt{E/F_{yf}}$ and $1.66\sqrt{E/F_{yf}}$ (8, 17, 24 and 40, respectively, for $F_{yf} = 50$ ksi) and h/t_w values of $0.50\sqrt{E/F_{yw}}$, $0.66\sqrt{E/F_{yw}}$, $1.00\sqrt{E/F_{yw}}$ and $1.49\sqrt{E/F_{yw}}$ (12, 16, 24 and 36, respectively, for $F_{yw} =$ 50 ksi)—all with a flange and web yield stresses of 50 ksi. Both stiffened and unstiffened link models were analyzed for each combination of cross-sectional parameters and lengths, where the stiffeners were external stiffeners (similar to those shown in Figure 1b) that satisfied the spacing requirement of Equation 23.

Results of the part A analyses are summarized in Figure 5. As shown, stiffened and unstiffened links of all lengths with

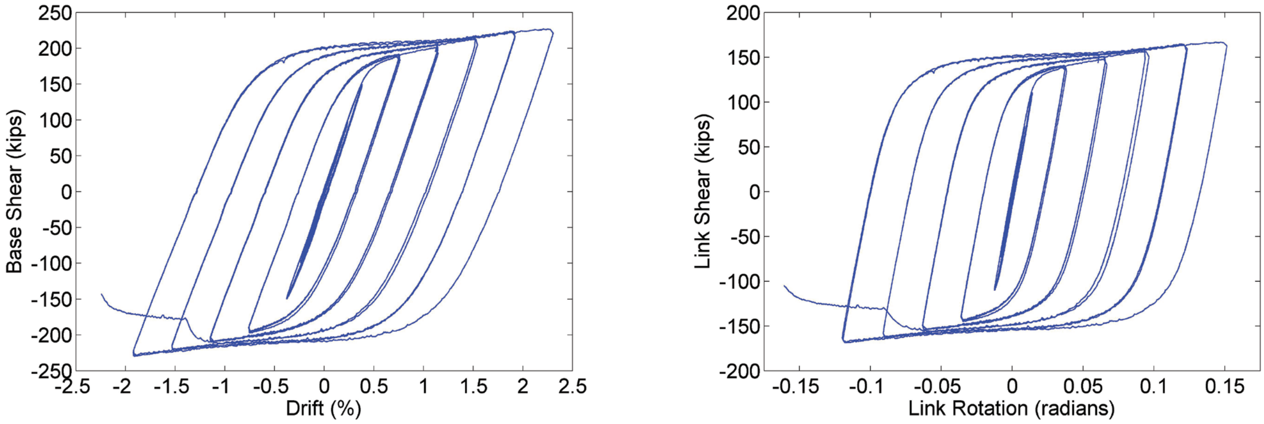

(a) *(b)*

Fig. 4. Large-scale EBF with built-up box link experimental results: (a) base shear versus drift; (b) link shear force versus link rotation angle (adapted from Berman and Bruneau, 2005).

$b/t_f \le 0.71\sqrt{E/F_{yf}}$ and $h/t_w \le 0.66\sqrt{E/F_{yw}}$ had maximum plastic rotations above the limit plastic rotations per the 2002 AISC *Seismic Provisions*, identified as the solid line in the figures. Furthermore, all stiffened links with $e \le 1.6M_p/V_p$ had maximum plastic rotations above the limit plastic rotations per the 2002 AISC *Seismic Provisions* for all considered h/t_w values when $b/t_f \le 0.71\sqrt{E/F_{yf}}$. There were three exceptions: two links with lengths of $2.1M_p/V_p$ and one with $1.6M_p/V_p$. The maximum rotations for those links were within 3% of the limit rotations per the 2002 AISC *Seismic Provisions,* and when they were reanalyzed with a slightly larger flange thickness such that $b/t_f = 0.64\sqrt{E/F_{yf}}$, they developed maximum rotations that exceeded the specified limit rotations. Additional analyses described in Berman and Bruneau (2006) were conducted for unstiffened links with $e \le 1.6M_p/V_p$ and $h/t_w = 1.67\sqrt{E/F_{yw}}$ by increasing the web yield stress. Those links were also found to have adequate plastic rotation capacity. Based on the preceding results, the recommendations for links with built-up box sections in the companion technical note (Bruneau, 2013) were established as follows:

1. All links should have $b/t_f \le 0.64\sqrt{E/F_{yf}}$.
2. Links with length $e > 1.6M_p/V_p$ do not require stiffeners and should have $h/t_w \le 0.64\sqrt{E/F_{yw}}$.
3. Links with length $e \le 1.6M_p/V_p$ should have $h/t_w \le 1.67\sqrt{E/F_{yw}}$. They may be unstiffened if $h/t_w \le 0.64\sqrt{E/F_{yw}}$ and should have stiffeners meeting the spacing requirements of Equation 23 if $h/t_w > 0.64\sqrt{E/F_{yw}}$.

Note that flange stiffeners were found to be ineffective in preventing flange buckling. Thus, only web stiffeners are necessary when stiffeners are required, making it possible to place them inside the built-up box section to improve constructability and architectural appeal. Additionally, Figure 5 indicates that for links with lengths greater than $2.1M_p/V_p$, web width-to-thickness ratios greater than $0.66\sqrt{E/F_{yw}}$ are able to achieve their target rotation. An upper bound for web depth-to-thickness for long links was not found as part of this research and could be the subject of future investigation.

Part B of the finite element parametric study consisted of models with webs and flanges proportioned to be just at the upper bounds of the previously recommended plate slenderness limits, with web and flange yield stresses ranging from 36 to 65 ksi. The four link lengths of $1.2M_p/V_p$, $1.6M_p/V_p$, $2.1M_p/V_p$ and $3.0M_p/V_p$ were again considered, and all links were found to have adequate plastic rotation capacity to satisfy the limits in the AISC *Seismic Provisions.*

The preceding recommendations are logical considering the state of stress in the webs and flanges of links with various lengths. For short links, shear yielding of the webs occurs first, and large plastic shear strains in the web require stiffeners to prevent web buckling when h/t_w is large. As strain hardening occurs in the webs, which is more rapid for cyclic shear yielding relative to cyclic yielding under normal stress, the shear force increases, resulting in larger link end moments to maintain equilibrium and correspondingly larger compressive stress in the flanges. Thus, flange buckling is not only a concern for longer links that yield primarily flexure but also for shorter links that yield first in shear. For longer links, the shear stress in the web is lower, and instead, the web may carry considerable flexural compression and tension stresses. Web buckling under this flexural compression is likely for longer links, and vertical web stiffeners are ineffective to prevent such buckling. Therefore, long links require a smaller h/t_w.

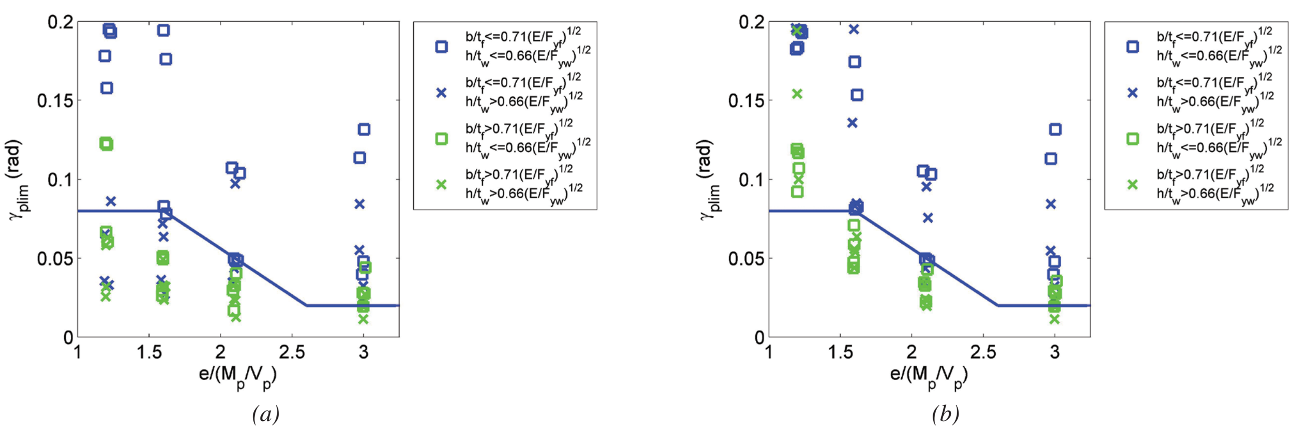

Fig. 5. Finite element modeling results: plastic rotation versus normalized link length for (a) unstiffened links and (b) stiffened links (data from Berman and Bruneau, 2006).

To verify the results of the finite element parametric study, tests on 14 links with built-up box sections were performed and are described in detail in Berman and Bruneau (2008b). The test setup is shown Figure 6 along with the two typical link schematics. Twelve of the links had haunches at their ends to reinforce the connections to the end plates. Two of the links had end details with gusset plates simulating the brace connections used in the full-scale proof-of-concept test, which is a detail more typical of what may be used in an actual EBF implementation. In both cases, the link length is the free length between the end connections as shown in Figure 6.

Flange fracture due to low-cycle fatigue was the governing limit state and the primary cause of strength degradation in all specimens. Although some evidence of moderate web and/or flange buckling was observed in some cases, there was little strength degradation associated with it. This does indicate that flange fracture must be guarded against when detailing the eccentric brace connections to the link, and designers should opt for details that minimize the restraint against flange deformation there. Flange fracture was not simulated in the finite element studies, but a similar failure mode was observed in the full-scale, single-story story test after the link achieved large rotations.

During the testing of the isolated links, the 2005 AISC *Seismic Provisions* were released. They contained a new recommended loading protocol for EBF links based on work by Richards and Uang (2006). The new loading protocol featured more cycles at smaller rotation levels and fewer cycles at larger rotation levels, resulting in less cumulative plastic

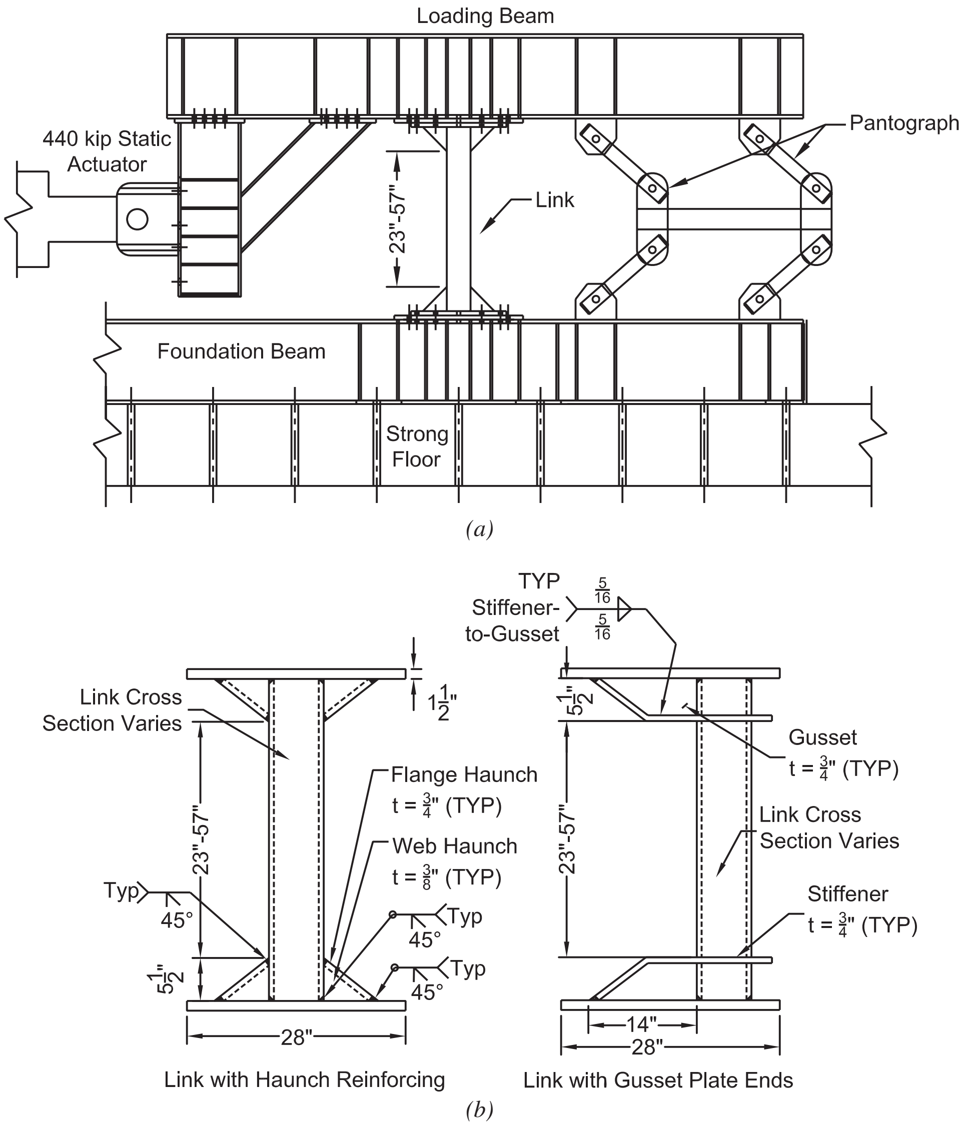

Fig. 6. Isolated link tests: (a) experimental setup; (b) typical link configurations (adapted from Berman and Bruneau, 2006).

rotation required to reach the limit plastic rotations. Thirteen of the links were tested under the older, more demanding loading protocol, while one was tested under the newer loading protocol, the latter having identical details as one of the links from the group of 13. The link tested under the new protocol achieved a considerably larger plastic rotation than that achieved with the older loading protocol. The maximum plastic rotations achieved by links tested under the older loading protocol were then projected to maximum plastic rotations that would likely have been achieved under the newer loading protocol using cumulative plastic rotation as the basis for this conversion, as described in Berman and Bruneau (2008b). The resulting projected link plastic rotations are shown in Figure 7 versus the normalized link length, $e/(M_p/V_p)$. The results from the full-scale, single-story EBF test are also included. As shown, all links that meet the proposed design requirements achieved their limit plastic rotations as specified in the 2005 AISC *Seismic Provisions* when the updated loading protocol is considered.

SUMMARY, CONCLUSIONS AND RECOMMENDATIONS

An analytical and experimental study of EBF links built-up box sections was performed to develop design recommendations, including lateral bracing conditions, flange width-to-thickness and web width-to-thickness limits, and stiffener spacing requirements. The study consisted of a derivation of some design requirements, large-scale testing of a single-story EBF with a built-up box link, a parametric study using finite element analyses of built-up box links with various section dimensions, and an experimental study on isolated links having various sections properties and plate slenderness ratios. In general, links with built-up box sections performed adequately and were able to meet the ductility requirements for use in EBFs, as long as the proposed width and width-to-thickness ratio limits were satisfied.

A flange width-to-thickness ratio limit was derived considering plate buckling equations, but it was shown to be unconservative by finite element analysis results that considered cyclic plastic deformation of the flanges. Web stiffener spacing requirements were derived using methods similar to those used for stiffener requirements for links with I-shaped sections and were found to be adequate by the results from the finite element analyses and experiments. An upper limit on web width-to-thickness ratio was established via the finite element parametric study. Lateral bracing was not used for the link or beam in the full-scale, single-story EBF test, and no evidence of lateral instability was observed. Based on the cumulative results of the study, the design requirements for EBF links with built-up sections are:

1. All links should have $b/t_f \le 0.64\sqrt{E/F_{yf}}$.
2. Links with length $e > 1.6M_p/V_p$ do not require stiffeners and should have $h/t_w \le 0.64\sqrt{E/F_{yw}}$.
3. Links with length $e \le 1.6M_p/V_p$ should have $h/t_w \le 1.67\sqrt{E/F_{yw}}$. They may be unstiffened if $h/t_w \le 0.64\sqrt{E/F_{yw}}$ and should have web stiffeners if $h/t_w > 0.64\sqrt{E/F_{yw}}$.

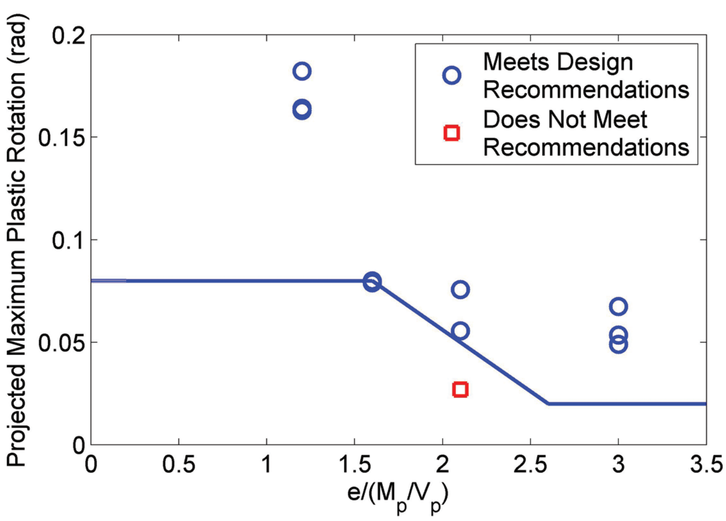

Fig. 7. Isolated link test results, projected maximum plastic rotation versus normalized link length (data from Berman and Bruneau, 2006).

4. Where web stiffeners are required they should be spaced at a spacing, a, no larger than:

$$a = C_B t_w - \frac{h}{8} \tag{23}$$

   where C_B is 20 and 37 for maximum link rotations of 0.08 and 0.02 rad, respectively. Linear interpolation may be used for other link rotation angles.

5. Lateral bracing of links with built-up box sections is unlikely to be necessary.

ACKNOWLEDGMENTS

This research was conducted by the State University of New York at Buffalo and was supported by the Federal Highway Administration under Contract No. DTFH61-98-C-00094 and the Multidisciplinary Center for Earthquake Engineering Research. However, any opinions, findings, conclusions and recommendations presented in this paper are those of the writers and do not necessarily reflect the views of the sponsors.

REFERENCES

AISC (2002), *Seismic Provisions for Structural Steel Buildings,* AISC 341-02, American Institute of Steel Construction, Chicago, IL.

AISC (2005), *Seismic Provisions for Structural Steel Buildings,* AISC 341-05, American Institute of Steel Construction, Chicago, IL.

AISC (2010), *Seismic Provisions for Structural Steel Buildings,* AISC 341-10, American Institute of Steel Construction, Chicago, IL.

Basler, K., (1961), "Strength of Plate Girders in Shear," *Journal of the Structural Division*, ASCE, Vol. 87, No. 7, pp. 150–180.

Berman, J.W. and Bruneau, M. (2005), "Approaches for the Seismic Retrofit of Braced Steel Bridge Piers and Proof-of-Concept Testing of a Laterally Stable Eccentrically Braced Frame," Technical Report No. MCEER-05-0004, Multidisciplinary Center for Earthquake Engineering Research, Buffalo, NY.

Berman, J.W. and Bruneau, M. (2006), "Further Development of Tubular Eccentrically Braced Frame Links for the Seismic Retrofit of Braced Steel Truss Bridge Piers," Technical Report No. MCEER-06-0006, Multidisciplinary Center for Earthquake Engineering Research, Buffalo, NY.

Berman, J.W. and Bruneau, M. (2007), "Experimental and Analytical Investigation of Tubular Links for Eccentrically Braced Frames," *Engineering Structures*, Vol. 29, No. 8, pp. 1929–1938.

Berman, J.W. and Bruneau, M. (2008a), "Tubular Links for Eccentrically Braced Frames I: Finite Element Parametric Study," *Journal of Structural Engineering*, ASCE, Vol. 134, No. 5, pp. 692–701.

Berman, J.W. and Bruneau, M. (2008b), "Tubular Links for Eccentrically Braced Frames II: Experimental Verification," *Journal of Structural Engineering*, ASCE, Vol. 134, No. 5, pp. 702–712.

Bruneau, M. (2013), "Setting Limits," *Modern Steel Construction,* February.

Galambos, T.V. (1998), *Guide to Stability Design Criteria for Metal Structures*, John Wiley and Sons, New York, NY.

Haaijer, G. (1957), "Plate Buckling in the Strain-Hardening Range," *Journal of the Engineering Mechanics Division*, Vol. 83, No. 2, pp. 1212-1 – 1212-47.

Hassan, O.F. and Goel, S.C. (1991), "Modeling of Bracing Members and Seismic Behavior of Concentrically Braced Steel Structures," Technical Report UMCE 91-1, University of Michigan Department of Civil Engineering, Ann Arbor, MI.

Kasai, K. and Popov, E.P. (1986), "Study of Seismically Resistant Eccentrically Braced Steel Frame Systems," Report No. UCB/EERC-86/01, Earthquake Engineering Research Center, College of Engineering, University of California, Berkeley, CA.

Lee, S. and Goel, S.C. (1987), "Seismic Behavior of Hollow and Concrete-Filled Square Tubular Members," Technical Report UMCE 87-11, University of Michigan Department of Civil Engineering, Ann Arbor, MI.

Richards, P. and Uang, C. M. (2006). "Testing Protocol for Short Links in Eccentrically Braced Frames," *Journal of Structural Engineering*, ASCE, Vol. 132, No. 8, pp. 1183–1191.

Roeder, C.W. and Popov, E.P. (1977), "Inelastic Behavior of Eccentrically Braced Steel Frames Under Cyclic Loadings," Report No. UCB/EERC-77/18, Earthquake Engineering Research Center, College of Engineering, University of California, Berkeley, CA.

A Comparison between the 2005 and 2010 AISC Specification

ERIC J. BOLIN, THOMAS J. DEHLIN and LOUIS F. GESCHWINDNER

ABSTRACT

In 2010, the American Institute of Steel Construction published a revised version of its *Specification for Structural Steel Buildings* that replaces the 2005 edition. Changes to the *Specification* were minimal and improved the usability and accuracy of the document. A detailed summary of these changes are contained in this article, providing an extension to the historical reviews of previous AISC specifications presented in Appendix A1 of AISC Design Guide 15.

Keywords: design specifications.

INTRODUCTION

The American Institute of Steel Construction and its Committee on Specifications make great efforts to ensure that the AISC *Specification for Structural Steel Buildings* is presented in a manner that is as clear and simple as possible. Since the first edition was first adopted in 1923, the *Specification* has been revised periodically with the intent to broaden its scope, simplify design procedures, improve the accuracy of some provisions and improve its usability. The 2010 edition continues this advancement of the *Specification* with a few new changes.

To assist users of previous editions of the *Specification* with the newest changes, a cross-reference list has been prepared here, detailing the specific changes made to each provision. This list contains the changes in both content and organization between the 2010 and 2005 editions of the *Specification*. This list expands the historical review found in Appendix A1 of AISC Design Guide 15 (Brockenbrough, 2002) of AISC Specifications and corresponding Supplements from the first edition published in 1923 through the most current 2010 edition. AISC has made the 2010 *Specification* available for free download through the AISC website at www.aisc.org/epubs, but it can also be found in Part 16 of the 14th edition of the AISC *Steel Construction Manual*.

Three major changes that are evident upon using the new *Specification* include a new Chapter N, a major reorganization of Chapters I and K and an increase in the nominal bolt shear strength tabulated in Chapter J.

Eric J. Bolin, Project Engineer, Drucker Zajdel Structural Engineers, Inc., Naperville, IL (corresponding author). E-mail: eric@dzse.com

Thomas Dehlin, Graduate Research Assistant, University of Illinois at Urbana-Champaign, Urbana, IL. E-mail: tdehlin90@gmail.com

Louis F. Geschwindner, Ph.D., P.E., Professor Emeritus of Architectural Engineering, The Pennsylvania State University, University Park, PA. E-mail: lfg@psu.edu

Chapter N, "Quality Control and Quality Assurance," is a compilation of the quality control provisions in Chapter M of the 2005 *Specification* and the quality assurance provisions in various other documents. Chapter N was added to the 2010 *Specification* as a means of tying all of these elements of quality control and assurance together in a consistent, uniform plan. There is little, if anything, in Chapter N that creates a new requirement—rather, this chapter creates an awareness of requirements that have existed elsewhere already, and it generally makes reference to those requirements in "roadmap" form.

Most of Chapter I, "Design of Composite Members," has been reorganized and improved in the newest edition of the *Specification*. Several new topics are covered in this chapter, including design and detailing of composite diaphragms and collector beams, shear and tension interaction strength of steel headed stud anchors (a.k.a., shear stud connectors) and the classification for local buckling of filled composite members.

The provisions within Chapter K, "Design of HSS and Box Member Connections," have been mostly reorganized into a tabular format with figures showing different connection configurations and their respective limit states.

In Chapter J, "Design of Connections," the nominal bolt shear strength for bolts in bearing-type connections has increased by approximately 12.5% for most cases, allowing for a more efficient connection design if bolt shear is the controlling limit state.

The following summarizes the revisions contained in the 2010 AISC *Specification for Structural Steel Buildings* (ANSI/AISC 360-10) compared to the 2005 AISC *Specification for Structural Steel Buildings* (ANSI/AISC 360-05). The organization of the summary parallels the format of the 2010 AISC *Specification*. For full details on the various changes, reference should be made to the 2010 AISC *Specification*.

CHAPTER A
GENERAL PROVISIONS

The major changes to this chapter include:

- Minor editorial changes have been made.
- Several new reference standards, codes and specifications have been added.

A1. SCOPE

The scope statement of the 2010 *Specification* has been expanded by including other structures (through reference to the AISC *Code of Standard Practice for Steel Buildings and Bridges*) and systems with structural steel acting compositely with reinforced concrete. These systems had always been included in the *Specification* but had not been listed separately in this section. Clarification has been added that whenever the *Specification* refers to the applicable building code and there is none, ASCE/SEI 7 is to be used for loads, load combinations, system limitations and general design requirements. This broadens what is already given in Section B2.

A1.1. Seismic Applications (was Sections A1.1 and A1.2)

The *Seismic Provisions for Structural Steel Buildings* (ANSI/AISC 341) apply for the design of seismic force resisting systems unless exempted by the building code. Thus, the discussion of low-seismic applications and high-seismic applications was deleted. Further, the discussion of the seismic response modification factor, *R*, has been moved into a new user note.

A1.2. Nuclear Applications (was Section A1.3)

The reference to the *Load and Resistance Factor Design Specification for Steel Safety-Related Structures for Nuclear Facilities* (ANSI/AISC N690L) has been removed from this section because it has been superseded.

A2. REFERENCED SPECIFICATIONS, CODES AND STANDARDS

Several additions and updates have been made to the specifications, codes and standards listed in this section.

A3. MATERIAL

A3.1. Structural Steel Materials

The following statement has been removed from this section, "If requested, the fabricator shall provide an affidavit stating that the structural steel furnished meets the requirements of the grade specified."

A3.1a. ASTM Designations

Several ASTM specifications have been added as approved for use with the 2010 *Specification*. In addition, metric standards for already approved materials have been included. The following materials have been added:

- Hot-rolled shapes—ASTM A1043/A1043M
- Structural tubing—ASTM 618M and A847M
- Plates—ASTM A1043/1043M
- Sheets—ASTM A606M

A3.1b. Unidentified Steel

This section is expanded to clarify the intent of the term "unimportant." It now includes a statement that the use of unidentified steel shall be subject to the approval of the engineer of record.

A3.1c. Rolled Heavy Shapes

The exception has been changed as follows:

- 2005 *Specification*: Charpy V-notch results are not required when a non-heavy shape is welded to the face of a rolled heavy shape with complete joint penetration groove welds.
- 2010 *Specification*: When a rolled heavy shape is welded to the surface of another shape using groove welds, the Charpy V-notch requirement only applies to the shape with the weld metal fused through the cross-section.

A3.1d. Built-Up Heavy Shapes

No changes have been made to this section.

A3.2. Steel Castings and Forgings

No changes have been made to this section.

A3.3. Bolts, Washers and Nuts

The following ASTM specifications have been added for bolts: ASTM A354 and ASTM F2280. For washers, ASTM F844 has been added.

A3.4. Anchor Rods and Threaded Rods

No changes have been made to this section.

A3.5. Consumables for Welding

The title of this section has been changed from "Filler Metal Flux for Welding." The metric-equivalent American Welding Society specifications are now listed for all approved consumables.

A3.6. Headed Stud Anchors

The title of this section has been changed from "Stud Shear Connectors." Steel stud shear connectors are now called steel-headed stud anchors. The metric-equivalent welding code, AWS D1.1M, was added to this section. The user note referencing ASTM A29/A29M-04 for studs made from cold drawn bar has been removed.

A4. STRUCTURAL DESIGN DRAWINGS AND SPECIFICATIONS

The provision requiring that deviations from the *Code of Standard Practice for Steel Buildings and Bridges* be specifically identified in design drawings and/or specifications has been removed. A user note is added to this section stating the information that is to be shown on the design drawings.

CHAPTER B
DESIGN REQUIREMENTS

The major changes to this chapter include:

- Structural integrity requirements for connections in the limit state section have been incorporated.
- The moment redistribution section has been moved to this chapter from Appendix 1.
- A section for the design of diaphragms and collectors has been added.
- The tables for limiting width-to-thickness ratios for flexure and compression elements have been reorganized.
- A new section has been added with changing language for quality control and quality assurance provisions.

B1. GENERAL PROVISIONS

No changes have been made to this section.

B2. LOADS AND LOAD COMBINATIONS

The user note in this section has been reworded for clarity.

B3. DESIGN BASIS

Several new sections have been added. Section B3.12, "Design Wall Thickness for HSS," has been moved to Section B4.2. Section B3.13, "Gross and Net Area Determination," has been moved to Section B4.3.

B3.1. Required Strength

The reference to the provisions in Appendix 1 for moment redistribution in continuous beams has been removed because this topic has been moved into this chapter.

B3.2. Limit States

Treatment of limit states when meeting structural integrity requirements have been added. The limit states intended to limit deformations or yielding are not considered for satisfying structural integrity requirements. Bolt bearing with short-slotted holes parallel to the direction of tension is permitted.

B3.3. Design for Strength Using Load and Resistance Factor Design (LRFD)

No changes have been made to this section.

B3.4. Design for Strength Using Allowable Strength Design (ASD)

No changes have been made to this section.

B3.5. Design for Stability

No changes have been made to this section.

B3.6. Design of Connections

For clarification, the statement that self-limiting inelastic deformations are permitted has been added to this section to apply to all connections. At points of support, beams, girders and trusses must be restrained against rotation about their longitudinal axis unless analysis shows that restraint is not required. This is to clarify the requirements that exist in Chapter F.

B3.6a. Simple Connections

The provision permitting inelastic rotation of a connection has been removed because it is now addressed directly in Section B3.6.

B3.6b. Moment Connections

No changes have been made to this section.

B3.7. Moment Redistribution in Beams (new section, was Appendix 1, Section 1.3)

A limitation has been added that does not permit moment redistribution when using partially restrained moment connections.

B3.8. Diaphragms and Collectors (new section)

This section is used to remind designers that these elements must be designed.

B3.9. Design for Serviceability (was Section B3.7)

This section was edited for clarity.

B3.10. Design for Ponding (was Section B3.8)

No changes have been made to this section.

B3.11. Design for Fatigue (was Section B3.9)

No changes have been made to this section.

B3.12. Design for Fire Conditions (was Section B3.10)

This section was edited for clarity.

B3.13. Design for Corrosion Effects (was Section B3.11)

No changes have been made to this section.

B3.14. Anchorage to Concrete (new section)

This section includes charging language for design of anchorage between steel and concrete acting compositely and for design of column bases and anchor rods.

B4. MEMBER PROPERTIES

The title of this section has been changed from "Classification of Sections for Local Buckling" due to the expanded coverage of this section. Several subsections have been moved here including, B4.2, "Design Wall Thickness for HSS," and B4.3, "Gross and Net Area Determination."

B4.1. Classification of Sections for Local Buckling (was Section B4)

To clarify the distinction between columns and beams and to eliminate the notation "NA" for λ_p (which is not applicable to columns), the local buckling classifications have been separated for flexure and compression. The classification for flexure remains compact/noncompact/slender, while compression members are now classified as nonslender/slender. Table B4.1 has been divided into two parts, Tables B4.1a for members subject to axial compression and B4.1b for members subject to flexure.

B4.1a. Unstiffened Elements (was Section B4.1)

No changes have been made to this section.

B4.1b. Stiffened Elements (was Section B4.2)

Section (e) has been added, defining b, the width of perforated cover plates.

TABLE B4.1a
Width-to-Thickness Ratios: Compression Elements Members Subject to Axial Compression

This table contains the cases from Table B4.1 in the 2005 *Specification* that apply to compression. New figures are included in the "Examples column," which now illustrate a larger number of possibilities. Because compression elements in members subject to axial compression are either nonslender or slender, only the limiting width-to-thickness ratio, λ_r, is provided in Table B4.1a. The following table shows the changes that have been made to the element descriptions and the case numbering in this table.

Case (2010)	Case (2005)	Change in Description
1	3	Flanges of tees have been added to this case.
2	4	*
3	5	*
4	8	*
5	10	Channels have been added to this case.
6	12	Flanges have been changed to walls and bending moved to Table B4.1b.
7	12	Bending moved to Table B4.1b.
8	14	*
9	15	Circular hollow sections have been changed to round HSS and bending moved to Table B4.1b.

* No changes have been made.

TABLE B4.1b
Width-to-Thickness Ratios: Compression Elements Members Subject to Flexure

This table contains the cases from Table B4.1 in the 2005 *Specification* that apply to flexure. New figures are included in the "Examples" column, which now illustrate a larger number of possibilities. The following table shows the changes that have been made to the element descriptions and case numbering in Table B4.1b.

Case (2010)	Case (2005)	Change in Description
10	1,7	*
11	2	*
12	6	*
13	1	Clarification for weak axis flexure.
14	New	New provisions for the stems of tees in flexure.
15	9	*
16	11	*
17	12	Compression moved to Table B4.1a.
18	12	Compression moved to Table B4.1a.
19	13	Webs of boxes added.
20	15	Circular hollow sections has been changed to round HSS and compression moved to Table B4.1a.

* No changes have been made.

B4.2. Design Wall Thickness for HSS (was Section B3.12)
No changes have been made to this section.

B4.3. Gross and Net Area Determination (was Section B3.13)

B4.3a. Gross Area (was Section B3.13a)
No changes have been made to this section.

B4.3b. Net Area (was Section B3.13b)
The reference to Section J3.2 for determining hole and slot dimensions was removed because it was unnecessary. For clarity, the following statement has been added: "For members without holes, the net area, A_n, is equal to the gross area, A_g."

B5. FABRICATION AND ERECTION
Quality control was moved to Section B6.

B6. QUALITY CONTROL AND QUALITY ASSURANCE (new section)
This new section contains the charging language for the new Chapter N, "Quality Control and Quality Assurance."

B7. EVALUATION OF EXISTING STRUCTURES (was Section B6)
This section has been reworded for clarity.

CHAPTER C
DESIGN FOR STABILITY

The major changes to this chapter include:

- The title of this chapter has been changed from "Stability Analysis and Design."
- This chapter now contains the direct analysis method, which has been moved from Appendix.7
- The effective length method and the first-order analysis method have been moved to Appendix 7.
- The approximate second-order analysis method (B_1-B_2 method) has been moved to Appendix 8.
- A new section, C3, titled "Calculation of Available Strengths," has been added to this chapter.

C1. GENERAL STABILITY REQUIREMENTS (was Section C1.1)
The content of this section has been reorganized for clarity. A numbered list is now provided for effects that must be considered when assessing the stability of a structure. Consideration of residual

stresses has been expanded to include stiffness reduction due to inelasticity. Uncertainty in stiffness and strength has been added as a consideration. The LRFD and ASD load levels used for analysis are added to this section. A user note is included in this section defining the term "design," which is the combination of analysis to determine required strength and proportioning components to have adequate available strength.

C1.1. Direct Analysis Method of Design (new section)

This section permits the use of the direct analysis method for all structures.

C1.2. Alternative Methods of Design (new section)

This section permits the use of the effective length method and the first-order analysis method, defined in Appendix 7, when meeting the constraints specified. Appendix 7 contains the material on these methods that had been in Chapter C.

C2. CALCULATION OF REQUIRED STRENGTHS

This section now contains the required strength calculations using the direct analysis method. The content of this section has been moved from Appendix 7 in the 2005 *Specification* so all sections are new; however, the material is generally not new.

C2.1. General Analysis Requirements (new section)

The conditions under which the influence of P-δ effects on the response of the structure may be neglected have been expanded. Two user notes have been added; one states the that P-δ effects evaluated for individual members can be satisfied by applying the B_1 multiplier, and the other states that all gravity loads should be included in the analysis.

C2.2. Consideration of Initial Imperfections (new section)

A user note has been added stating that the imperfections considered are the locations of points of intersection of members caused by the out-of-plumbness of columns and that initial out-of-straightness of members is addressed in Chapter E for compression members and is not considered explicitly in analysis.

C2.2a. Direct Modeling of Imperfections (new section)

A user note has been added stating the initial displacements should be similar in configuration to displacements caused by loading and buckling with magnitudes based on permissible construction tolerances given in the AISC *Code of Standard Practice*.

C2.2b. Use of Notional Loads to Represent Imperfections

The requirement that use of notional loads are permitted only for structures that support gravity loads primarily through nominally vertical members has been added. A user note has been added stating that using notional loads can create additional fictitious base shears and overturning moments. The correct horizontal reaction at the base is found using a force equal to but opposite in direction to the notional loads applied at the base.

C2.3. Adjustments to Stiffness (new section)

The reduced flexural stiffness and reduced axial stiffness equations have been deleted, and the requirements have been reformatted into a text description in order to clarify that the reduction applies to all stiffness contributing to the lateral load resistance of the structure. A paragraph has been added for the stability analysis of a structure using materials other than structural steel.

C3. CALCULATION OF AVAILABLE STRENGTHS (new section)

This section clarifies that Chapters D through K are used for determination of available strengths. It also includes the requirement, moved from Appendix 7.1, that the effective length factor, K, will be taken as unity unless a smaller value can be justified by analysis. A statement has been included reiterating the requirements of Appendix 6 that bracing that defines the unbraced length must have sufficient strength and stiffness. In addition, it is pointed out that bracing included in the second-order analysis, as required by the direct analysis method, need not meet the requirements of Appendix 6.

CHAPTER D
DESIGN OF MEMBERS FOR TENSION

The major changes to this chapter include:

- The gross and net area sections have been moved to Chapter B.
- A new minimum shear lag factor is given for open cross-section shapes.
- Modifications have been made to several of the descriptions of elements in Table D3.1.

D1. SLENDERNESS LIMITATIONS

No changes have been made to this section.

D2. TENSILE STRENGTH

No changes have been made to this section.

D3. EFFECTIVE NET AREA

The title of this section has been changed to reflect that gross area and net area provisions have been moved to Sections B4.3a and B4.3b, respectively. For open cross-sections, a minimum shear lag factor has been added. The requirement that connections be proportioned so that the shear lag factor need not be less than 0.60 unless eccentricity is included in the design has been removed.

TABLE D3.1
Shear Lag Factors for Connections to Tension Members

This table remains the same with the following exceptions: Case 2 has been expanded to include tension members that transmit tensile load with longitudinal welds in combination with transverse welds. Two new figures have been added for Case 2 examples. Case 8 is expanded to include double angles. In the 2005 *Specification,* the single-angle condition with two or three fasteners per line in the direction of loading, with $U = 0.60$, has been changed to only three fasteners and directs the user to Case 2 for fewer fasteners.

D4. BUILT-UP MEMBERS

No changes have been made to this section.

D5. PIN-CONNECTED MEMBERS

D5.1. Tensile Strength

No changes have been made to this section.

D5.2. Dimensional Requirements

No changes have been made to this section.

D6. EYEBARS

D6.1. Tensile Strength

No changes have been made to this section.

D6.2. Dimensional Requirements

No changes have been made to this section.

CHAPTER E
DESIGN OF MEMBERS FOR COMPRESSION

The major changes to this chapter include:

- A new user note table has been added to assist in determining the applicable sections in this chapter.

- Changes have been made to the provisions for single-angle compression members.
- A new modified slenderness ratio is given for built-up members.

E1. GENERAL PROVISIONS

Sections E1(a) and E1(b) have been removed from this section and new text is used throughout the chapter to clarify the applicability of the various limit states.

TABLE USER NOTE E1.1
Selection Table for the Application of Chapter E Sections
This new table shows the applicable limit states with chapter section references.

E2. EFFECTIVE LENGTH

The title of this section has been changed from "Slenderness Limitations and Effective Length" to reflect that it just defines the effective length factor. This section now references Appendix 7 (in addition to Chapter C) for the determination of the effective length factor, K.

E3. FLEXURAL BUCKLING OF MEMBERS WITHOUT SLENDER ELEMENTS

The title of this section has been changed from "Compressive Strength for Flexural Buckling of Members without Slender Elements." The flexural buckling stress, F_{cr}, is now referred to as the critical stress. In Section E3(a), the alternate slenderness check, $F_e \geq 0.44F_y$, is now shown as $F_y/F_e \leq 2.25$, and in Section E3(b), $F_e < 0.44F_y$, is now shown as $F_y/F_e > 2.25$ to eliminate the truncation of the coefficient. The definition of the elastic buckling stress, F_e, now references Appendix 7 instead of Section C2 because that material was moved.

E4. TORSIONAL AND FLEXURAL-TORSIONAL BUCKLING OF MEMBERS WITHOUT SLENDER ELEMENTS

The title of this section has been changed from "Compressive Strength for Torsional and Flexural-Torsional Buckling of Members without Slender Elements." This section now clearly states that it applies to all doubly symmetric members without slender elements when the torsional unbraced length exceeds the lateral unbraced length and for single angles with $b/t > 20$ as a clarification for what was removed from Sections E1(a) and E1(b). In Section E4(a), the definition of member slenderness for double-angle compression members is clarified. With the exception of their organization, the equations in this section remain unchanged.

E5. SINGLE-ANGLE COMPRESSION MEMBERS

This section now stipulates that the provisions in Section E4 apply to single angles with $b/t > 20$. The material in Section E5(c) has been moved to Section E5, with the exception of the specific examples of different end conditions requiring the use of Chapter H provisions, which have been removed.

E6. BUILT-UP MEMBERS

E6.1. Compressive Strength

This section has been reorganized for clarity. The requirement that the end connection of built-up members be welded or connected by means of pretensioned bolts with Class A or B faying surfaces has been moved here from Section E6.2. The user note from Section E6.2 has also been moved into this section. This user note has added that the end connection should be designed to resist slip. Section E6.1(i) has been changed to E6.1(a), and Section E6.1(ii) has been changed to E6.1(b). In Section E6.1(b), the modified column slenderness equation for built-up shapes with intermediate connectors that are welded or connected with pretensioned bolts has been replaced with two new equations.

E6.2. Dimensional Requirements

Parts of this section have been reworded for clarity.

E7. MEMBERS WITH SLENDER ELEMENTS

A statement that it is conservative to use the smaller Q_s for cross-sections composed of multiple unstiffened slender elements has been added to the user note.

E7.1. Slender Unstiffened Elements, Q_s

In Section E7.1(b), the referenced member was changed from built-up to built-up I-shaped.

E7.2. Slender Stiffened Elements, Q_a

No changes have been made to this section.

CHAPTER F
DESIGN OF MEMBERS FOR FLEXURE

The major changes to this chapter include:

- The equation for the lateral-torsional buckling modification factor, C_b, has been modified.
- The equations for flange local buckling of tees have been modified.
- A new section for the limit state of local buckling of tee stems has been added.
- New proportioning limits are now given for I-shaped members.
- This chapter now contains the unbraced length requirement to permit moment redistribution.

TABLE USER NOTE F1.1
Selection Table for the Application of Chapter F Sections

The portion of this table referring to Section F12 for unsymmetrical shapes now excludes single angles.

F1. GENERAL PROVISIONS

The material addressing the lateral-torsional buckling modification factor has been separated into a new subsection. Application of the lateral-torsional buckling modification factor, C_b, as given is now limited to singly symmetric members in single curvature and all doubly symmetric members. In Equation F1-1, the cross-section monosymmetry parameter, R_m, has been removed along with the upper limit. The statement that C_b is permitted to be conservatively taken as 1.0 has been removed. The user note has been expanded to include a reference to the commentary for detailed analysis for singly symmetric members.

F2. DOUBLY SYMMETRIC COMPACT I-SHAPED MEMBERS AND CHANNELS BENT ABOUT THEIR MAJOR AXIS

F2.1. Yielding

No changes have been made to this section.

F2.2. Lateral-Torsional Buckling

A user note has been added stating that Equations F2-3 and F2-4 in the 2010 *Specification* produce results identical to the equations used in past editions of the LRFD *Specification*. Equation F2-6 has been reformatted to eliminate the issue when $J = 0$; otherwise, the equation produces identical results.

F3. DOUBLY SYMMETRIC I-SHAPED MEMBERS WITH COMPACT WEBS AND NONCOMPACT OR SLENDER FLANGES BENT ABOUT THEIR MAJOR AXIS

F3.1. Lateral-Torsional Buckling

No changes have been made in this section.

F3.2. Compression Flange Local Buckling

The definition of h has been clarified.

F4. OTHER I-SHAPED MEMBERS WITH COMPACT OR NONCOMPACT WEBS BENT ABOUT THEIR MAJOR AXIS

F4.1. Compression Flange Yielding

The definition of M_{yc} has been clarified.

F4.2. Lateral-Torsional Buckling

The web plastification factor, R_{pc}, for extreme singly symmetric members has been set to 1.0. The definitions for I_{yc} and h_c have been clarified.

F4.3. Compression Flange Local Buckling

No changes have been made to this section.

F4.4. Tension Flange Yielding

No changes have been made to this section.

F5. DOUBLY SYMMETRIC AND SINGLY SYMMETRIC I-SHAPED MEMBERS WITH SLENDER WEBS BENT ABOUT THEIR MAJOR AXIS

F5.1. Compression Flange Yielding

No changes have been made to this section.

F5.2. Lateral-Torsional Buckling

No changes have been made to this section.

F5.3. Compression Flange Local Buckling

No changes have been made to this section.

F5.4. Tension Flange Yielding

No changes have been made to this section.

F6. I-SHAPED MEMBERS AND CHANNELS BENT ABOUT THEIR MINOR AXIS

F6.1. Yielding

No changes have been made to this section.

F6.2. Flange Local Buckling

The definition of b has been clarified.

F7. SQUARE AND RECTANGULAR HSS AND BOX-SHAPED MEMBERS

A user note has been added to this section stating that a lateral-torsional buckling equation is not provided in this section because the limit state of beam deflection will control for reasonable cases.

F7.1. Yielding

No changes have been made to this section.

F7.2. Flange Local Buckling

No changes have been made to this section.

F7.3. Web Local Buckling

No changes have been made to this section.

F8. ROUND HSS

F8.1. Yielding

No changes have been made to this section.

F8.2. Local Buckling

No changes have been made to this section.

F9. TEES AND DOUBLE ANGLES LOADED IN THE PLANE OF SYMMETRY

A new section, F9.4, has been added to address the limit state of local buckling for tee stems in flexural compression.

F9.1. Yielding

New subsections have been added to improve clarity.

F9.2. Lateral-Torsional Buckling

No changes have been made to this section.

F9.3. Flange Local Buckling of Tees

The strength equations have been changed from stress to nominal moment and presented in a format similar to that for other shapes. A new user note has been added directing the user to Section F10.3 for double angles with flange legs in compression.

F9.4. Local Buckling of Tee Stems in Flexural Compression (new section)

The nominal moment strength of a tee stem in flexural compression is presented. This new approach replaces the past approach of relying on lateral-torsional buckling as the upper limit for flange local buckling. A user note has been included in this section for double angles with web legs in compression directing the user to Section F10.3.

F10. SINGLE ANGLES

For clarity, a requirement has been added stating that if there is moment about both principle axes with or without axial load, or if there is moment along one principle axis with axial load, the combined stress ratio shall be determined using Section H2. A user note has been added stating that if bending is about the minor axis, only the limit states of yielding and leg local buckling apply.

F10.1. Yielding

No changes have been made in this section.

F10.2. Lateral-Torsional Buckling

Several parts within this section have been relocated to improve organization, and Section F10.2(b)(iii) now indicates that no axial compression can be present.

F10.3. Leg Local Buckling

No changes have been made to this section.

F11. RECTANGULAR BARS AND ROUNDS

F11.1. Yielding

No changes have been made to this section.

F11.2. Lateral-Torsional Buckling

No changes have been made to this section.

F12. UNSYMMETRICAL SHAPES

No changes have been made to this section.

F12.1. Yielding

No changes have been made to this section.

F12.2. Lateral-Torsional Buckling

No changes have been made to this section.

F12.3. Local Buckling

No changes have been made to this section.

F13. PROPORTIONS OF BEAMS AND GIRDERS

F13.1. Strength Reductions for Members with Holes in the Tension Flange

This section has been renamed from "Hole Reductions." The references for area calculations have been changed appropriately.

F13.2. Proportioning Limits for I-Shaped Members

The maximum web slenderness ratio for I-shaped members with stiffened slender webs has been slightly revised.

F13.3. Cover Plates

No changes have been made to this section.

F13.4. Built-Up Beams

No changes have been made to this section.

F13.5. Unbraced Length for Moment Redistribution (new section)

The contents of this section have been moved here from Appendix 1, Section 1.7 in the 2005 *Specification*.

CHAPTER G
DESIGN OF MEMBERS FOR SHEAR

The major change to this chapter includes:

- A minimum moment of inertia of stiffeners for use with tension field action has been established.

G1. GENERAL PROVISIONS

No changes have been made to this section.

G2. MEMBERS WITH UNSTIFFENED OR STIFFENED WEBS

G2.1. Shear Strength

The title of this section has been changed from "Nominal Shear Strength," and the material has been edited for clarity.

G2.2. Transverse Stiffeners

A new variable, I_{st}, has been defined as the moment of inertia of transverse stiffeners, and the equation is now a function of the least dimension of the stiffened panel.

G3. TENSION FIELD ACTION

G3.1. Limits on the Use of Tension Field Action

No changes have been made to this section.

G3.2. Shear Strength with Tension Field Action

The title of this section has been changed from "Nominal Shear Strength with Tension Field Action."

G3.3. Transverse Stiffeners

The second limiting condition for stiffeners in tension field action has been changed from a basis on area to one on moment of inertia.

G4. SINGLE ANGLES

This section has been reorganized for clarity. The given, $C_v = 1.0$, has been removed, and for clarity, the web slenderness has been defined.

G5. RECTANGULAR HSS AND BOX-SHAPED MEMBERS

This section has been reorganized for clarity. The definition of the design wall thickness, t, has been added to this section.

G6. ROUND HSS

The definition of, A_g, has been changed from the gross area based on design wall thickness to the gross cross-sectional area of the member.

G7. WEAK AXIS SHEAR IN DOUBLY SYMMETRIC AND SINGLY SYMMETRIC SHAPES

Definitions have been added for clarity.

G8. BEAMS AND GIRDERS WITH WEB OPENINGS

No changes have been made to this section.

CHAPTER H
DESIGN OF MEMBERS FOR COMBINED FORCES AND TORSION

The major changes to this chapter include:

- A new section for the rupture of flanges with holes subject to tension has been added.
- For members subject to tension and flexure, the multiplier has been revised to be given in one equation for ASD and LRFD and the ASD constant changed from 1.5 to $\alpha = 1.6$.
- The interaction equation in Section H1.3 has been revised.

H1. DOUBLY AND SINGLY SYMMETRIC MEMBERS SUBJECT TO FLEXURE AND AXIAL FORCE

H1.1. Doubly and Singly Symmetric Members Subject to Flexure and Compression

No changes have been made to this section.

H1.2. Doubly and Singly Symmetric Members Subject to Flexure and Tension

The equation for the multiplier of C_b with doubly symmetric members using LRFD and ASD has been combined into a single equation. The use of α in this equation for ASD means that the constant has been changed from 1.5 to 1.6.

H1.3. Doubly Symmetric Rolled Compact Members Subject to Single Axis Flexure and Compression

The title of this section has been changed from "Doubly Symmetric Members in Single Axis Flexure and Compression." $(KL)_z \leq (KL)_y$ has been added as a limit on applicability to ensure that flexural buckling is the controlling limit state. The limit state of flexural-torsional buckling has been corrected to lateral-torsional buckling. The interaction equation for out-of-plane buckling has been revised. The statement that the moment ratio in Equation H1-2 shall be neglected if bending is only about the weak axis has been removed because this section only applies to bending about the major axis.

H2. UNSYMMETRIC AND OTHER MEMBERS SUBJECT TO FLEXURE AND AXIAL FORCE

Subscripts have been added for clarity.

H3. MEMBERS SUBJECT TO TORSION AND COMBINED TORSION, FLEXURE, SHEAR AND/OR AXIAL FORCE

The title of this section has been changed from "Members Under Torsion and Combined Torsion, Flexure, Shear and/or Axial Force."

H3.1. Round and Rectangular HSS Subject to Torsion

The title of this section has been changed from "Torsional Strength of Round and Rectangular HSS." This section has been reorganized, and definitions have been added for clarity.

H3.2. HSS Subject to Combined Torsion, Shear, Flexure and Axial Force

No changes have been made to this section.

H3.3. Non-HSS Members Subject to Torsion and Combined Stress

The title of this section has been changed from "Strength of Non-HSS Members Under Torsion and Combined Stress."

H4. RUPTURE OF FLANGES WITH HOLES SUBJECT TO TENSION (new section)

This new section has been added to address strength of flanges with holes subject to tension under combined axial force and major axis flexure.

CHAPTER I
DESIGN OF COMPOSITE MEMBERS

The major changes to this chapter include:

- The chapter has been extensively reorganized for clarity.
- The term "shear connector" has been changed to "steel-headed stud anchor."
- Limits on width-to-thickness ratios for filled composite members subject to compression and flexure have been expanded.
- Additional strength equations have been provided for filled composite members based on the new limiting width-to-thickness ratios.
- A single set of resistance and safety factors are now given for encased and filled composite members subject to flexure.
- Provisions for determining shear strength of filled and encased composite members are provided.
- New equations along with a set of resistance and safety factors are now given for direct bond interaction.
- Modifications have been made to the steel anchor detailing requirements for composite beams, and requirements for composite components have been added.
- A new section has been added for composite diaphragms and collector beams.
- The strength of steel-headed stud anchors in flat soffit slabs has been reduced.

I1. GENERAL PROVISIONS

The reference to the applicable building code and ACI 318 for the design, details and material properties of concrete and reinforcing steel have been moved to Section I1.1.

I1.1. Concrete and Steel Reinforcement (new section)

This section clarifies when ACI 318 is to be applied. A user note is included that indicates the intent of the *Specification* that the reinforced concrete portion of a composite section be detailed using the noncomposite provisions of ACI 318.

I1.2. Nominal Strength of Composite Sections (was Section I1.1)

A statement that local buckling effects need not be considered for encased members has been added.

I1.2a. Plastic Stress Distribution Method (was Section I1.1a)

Specific mention of concrete strength to be used in calculations has been removed and located in appropriate member design provisions.

I1.2b. Strain Compatibility Method (was Section I1.1b)

No changes have been made to this section.

I1.3. Material Limitations (was Section I1.2)

This section has been edited for clarity. The provision that higher strength materials are permitted when justified by testing or analysis has been removed, but it remains in the Commentary and is permitted by Section I9.

I1.4. Classification of Filled Composite Sections for Local Buckling (new section)

This section addresses the limiting width-to-thickness ratios for filled composite sections. The ratios and limits for filled composite members are presented in Tables I1.1a and I1.1b.

TABLE I1.1A
Limiting Width-to-Thickness Ratios for Compression Steel Elements in Composite Members Subject to Axial Compression for Use with Section I2.2 (new table)

Filled HSS and boxes in compression are defined as compact, noncompact or slender and a maximum permitted width-to-thickness ratio is established.

TABLE I1.1B
Limiting Width-to-Thickness Ratios for Compression Steel Elements in Composite Members Subject to Flexure for Use with Section I3.4 (new table)

Filled HSS and boxes in flexure are defined as compact, noncompact or slender and a maximum permitted width-to-thickness ratio is established.

I2. AXIAL FORCE

The title of this section has been changed from "Axial Members."

I2.1. Encased Composite Members

I2.1a. Limitations

A minimum size of lateral tie reinforcement has been added along with the maximum spacing based on reinforcement size and least column dimension. A user note is added clarifying that ACI 318 is to be used for additional tie and spiral reinforcement requirements.

I2.1b. Compressive Strength

For clarity, the provisions of this section have been revised to specifically apply to doubly symmetric encased composite members. Additionally, a statement has been added that the available compressive strength of the composite member need not be less than that of the bare steel member. The limits on the use of specific strength equations have been changed to be consistent with Section E3.

I2.1c. Tensile Strength

No changes have been made to this section.

I2.1d. Load Transfer (was Section I2.1e)

This section now refers to Section I6 for load transfer requirements for encased composite members.

I2.1e. Detailing Requirements (was Section I2.1f)

The requirement for total number of longitudinal reinforcing bars has been removed. The transverse reinforcement spacing requirement has been moved to Section I2.1a, and the requirements for shear connectors have been moved to Section I6. A provision for clear distance between reinforcing and the steel core has been added.

I2.2 Filled Composite Members

The title of this section has been changed from "Filled Composite Columns." Noncompact and slender members are now permitted by the provisions.

I2.2a. Limitations

The provisions now specifically apply to box members of uniform wall thickness as well as HSS. The width-to-thickness ratios for local buckling are contained in Table I1.1A. The maximum permitted *b/t* ratio for rectangular HSS and the maximum permitted *D/t* ratio for round HSS have been increased.

I2.2b. Compressive Strength

The strength equations have been revised to reflect the new provisions based on wall slenderness. For clarity, a statement has been added that the available compressive strength of the composite member need not be less that that of the bare steel member.

I2.2c. Tensile Strength

No changes have been made to this section.

I2.2d. Load Transfer

This section now refers to Section I6 for load transfer requirements for filled composite members.

I3. FLEXURE

The title of this section has been changed from "Flexural Members."

I3.1. General

I3.1a. Effective Width

No changes have been made to this section.

I3.1b. Strength During Construction (was Section I3.1c)

No changes have been made to this section.

I3.2. Composite Beams with Steel-Headed Stud or Steel Channel Anchors

The title of this section has been changed from "Strength of Composite Beams with Shear Connectors."

I3.2a. Positive Flexural Strength

No changes have been made to this section.

I3.2b. Negative Flexural Strength

No changes have been made to this section.

I3.2c. Composite Beams with Formed Steel Deck

The title of this section has been changed from "Strength of Composite Beams with Formed Steel Deck."

I3.2d. Load Transfer Between Steel Beam and Concrete Slab

The title of this section has been changed from "Shear Connectors." The subsections addressing strength of connectors have been moved to Section I8.

I3.3. Encased Composite Members

The title of this section has been changed from "Flexural Strength of Concrete-Encased and Filled Members." The provisions for filled members have been moved to Section I3.4. The resistance factor and safety factor is now the same regardless of the approach taken to calculating strength.

I3.4. Filled Composite Members (new section)

This topic has been moved from Section I3.3 and significantly expanded.

I3.4a. Limitations (new section)

Filled composite sections are now classified for local buckling using the limiting width-to-thickness ratios in Table I1.1B.

I3.4b. Flexural Strength (new section)

New equations have been provided for the calculation of the nominal flexural strength for compact, noncompact and slender filled composite members.

I4. SHEAR (new section)

I4.1. Filled and Encased Composite Members (was Sections I2.1d and I3.1b)

This section has combined the requirements for filled and encased beams and columns that had previously been presented separately. New resistance and safety factors are provided.

I4.2. Composite Beams with Formed Steel Deck (was Section I3.1b)

No changes have been made in these provisions.

I5. COMBINED FLEXURE AND AXIAL FORCE (was Section I4)

Provisions for composite beam-columns have been clarified and expanded.

I6. LOAD TRANSFER (new section)

I6.1. General Requirements (new section)

This section now combines the requirements for introduction and transfer of forces for both encased and filled axially loaded composite members.

I6.2. Force Allocation (was Section I2.1e)

These provisions now also apply to filled members.

I6.2a. External Force Applied to Steel Section (was Section I2.1e)

This section has been edited for clarity.

I6.2b. External Force Applied to Concrete (was Section I2.1e)

This section has been edited for clarity.

I6.2c. External Force Applied Concurrently to Steel and Concrete (new section)

This new section provides requirements for encased and filled composite members with force applied concurrently to the concrete and steel sections.

I6.3. Force Transfer Mechanisms (was Section I2.2e)

This section has been edited for clarity, and force transfer through direct bond interaction has been limited to filled composite members.

I6.3a. Direct Bearing (was Section I2.2e)

This section has been edited for clarity.

I6.3b. Shear Connection (new section)

This new section provides requirements for determination of strength of shear connectors in filled and encased composite members.

I6.3c. Direct Bond Interaction (new section)

This new section provides requirements for determination of strength for force transfer by direct bond interaction in filled rectangular and round composite members.

I6.4. Detailing Requirements (new section)

I6.4a. Encased Composite Members (was Section I2.1f)

The requirements for distribution of shear connectors has been changed from along the length of the member over a length of at least 2.5 times the depth of the member to within the load introduction length no greater than 2 times the minimum transverse dimension of the member.

I6.4b. Filled Composite Members (was Section I2.2f)

The requirements for distribution of the shear connectors has changed from along the length of the member at least 2.5 times the width or diameter of the HSS to within the load introduction length that shall not exceed 2 times the width of a rectangular steel member or 2 times the diameter of a round steel member. The provision for the maximum connector spacing of 16 in. has been moved to Section I8.3e and revised.

I7. COMPOSITE DIAPHRAGMS AND COLLECTOR BEAMS (new section)

This section requires that composite slab diaphragms and collector beams be designed.

I8. STEEL ANCHORS (was Section I3.2d)

The provisions in this section have been gathered from the previous provisions for composite beams and provisions for composite components have been added.

I8.1. General (was Section I3.2d(6))

This section has been edited for clarity.

I8.2. Steel Anchors in Composite Beams (was Section I1.3)

The title of this section has been changed from "Shear Connectors," and the section has been edited for clarity.

I8.2a. Strength of Steel-Headed Stud Anchors (was Section I3.2d(3))

The title of this section has been changed from "Strength of Stud Shear Connectors." For steel-headed stud anchors welded directly to the steel shape, the position effect factor, R_p, has been changed from 1.0 to 0.75.

I8.2b. Strength of Steel Channel Anchors (was Section I3.2d(4))

The title of this section has been changed from "Strength of Channel Shear Connectors," and the section has been edited for clarity.

I8.2c. Required Number of Steel Anchors (was Sections I3.2d(5) and (6))

This section has been edited for clarity.

I8.2d. Detailing Requirements (was Section I3.2d(6))

A provision for the minimum distance from the center of an anchor to a free edge in the direction of the shear force has been added.

I8.3. Steel Anchors in Composite Components (new section)

This new section provides requirements for all types of composite construction other than composite beams.

I8.3a. Shear Strength of Steel-Headed Stud Anchors in Composite Components (new section)

This section covers the shear strength of a steel headed stud anchor when concrete break-out is not an applicable limit state.

I8.3b. Tensile Strength of Steel-Headed Stud Anchors in Composite Components (new section)

This section covers the tensile strength of a steel-headed stud anchor based on the distance from the anchor to a free edge and the center-to-center anchor spacing.

I8.3c. Strength of Steel-Headed Stud Anchors for Interaction of Shear and Tension in Composite Components (new section)

This section covers the nominal strength for interaction between shear and tension for a steel-headed stud anchor.

I8.3d. Shear Strength of Steel Channel Anchors in Composite Components
(new section)

This section refers to Section I8.2b for strength of steel channel anchors and provides the resistance factor and safety factor for the steel channel anchors in composite components.

I8.3e. Detailing Requirements in Composite Components (new section)

This section establishes the minimum cover, minimum and maximum spacing of steel-headed stud anchors and maximum spacing of steel channel anchors for composite components.

I9. SPECIAL CASES (was Section I5)

No changes have been made to this section.

CHAPTER J
DESIGN OF CONNECTIONS

The major changes to this chapter include:

- Weld requirements have been revised where necessary to be consistent with AWS D1.1-2010.
- The base metal strength for partial-joint-penetration (PJP) groove welds in tension has been revised to use rupture strength rather than yield strength.
- To use provisions in Section J2.4 welds no longer need to be loaded in-plane.
- Bolt groups A and B have been established to simplify presentation of requirements for high-strength bolts.
- Nominal shear strength in bearing-type connections has been increased by approximately 12.5% for most cases.
- The resistance and safety factors for column bases and bearing on concrete have been changed.

J1. GENERAL PROVISIONS

J1.1. Design Basis

No changes have been made to this section.

J1.2. Simple Connections

No changes have been made to this section.

J1.3. Moment Connections

No changes have been made to this section.

J1.4. Compression Members with Bearing Joints

This section has been edited for clarity.

J1.5. Splices in Heavy Sections

A fourth provision, filler metal requirements as given in Section J2.6, has been added.

J1.6. Weld Access Holes

The title of this section has been changed from “Beam Copes and Weld Access Holes.” Beam cope provisions have been removed from this section.

A minimum length of 1½ in. has been added for access holes, and the minimum height has been changed from 1 in. to ¾ in.

J1.7. Placement of Welds and Bolts

No changes have been made to this section.

J1.8. Bolts in Combination with Welds

No changes have been made to this section.

J1.9. High-Strength Bolts in Combination with Rivets

No changes have been made to this section.

J1.10. Limitations on Bolted and Welded Connections

Slip-critical joints have been removed from the list of joints to which this section applies.

J2. WELDS

Many of the revisions to the weld requirements in this section have been made to be consistent with AWS D1.1/D1.1M-2010.

J2.1. Groove Welds

J2.1a. Effective Area

No changes have been made to this section.

TABLE J2.1
Effective Throat of Partial-Joint-Penetration Groove Welds

No changes have been made to this table.

TABLE J2.2
Effective Weld Throats of Flare Groove Welds

No changes have been made to this table.

TABLE J2.3
Minimum Effective Throat of Partial-Joint-Penetration Groove Welds

No changes have been made to this table.

J2.1b. Limitations

No changes have been made to this section.

J2.2. Fillet Welds

J2.2a. Effective Area

No changes have been made to this section.

J2.2b. Limitations

The actual length of the weld is now used instead of the effective length when establishing minimum length requirements for fillet welds designed on the basis of strength.

For all welds whose length exceeds 300 times its leg size, the effective length is now taken as 180 times its leg size instead of the former 0.6 times its length.

The clause "when the required strength is less than that developed by a continuous fillet weld of the smallest permitted size" has been removed from the paragraph outlining the conditions under which intermittent fillet welds may be used.

In addition to being used to transmit shear in lap joints, fillet welds in holes or slots are now permitted to be used to resist loads perpendicular to the faying surface in lap joints.

TABLE J2.4
Minimum Size of Fillet Welds

No changes have been made to this table.

J2.3. Plug and Slot Welds

J2.3a. Effective Area

No changes have been made to this section.

J2.3b. Limitations

No changes have been made to this section.

J2.4. Strength

The limit state of yielding has been removed as an applicable limit state. This deletion relates to tension strength of the base metal.

Welds are no longer required to be loaded in-plane to use the alternative provisions given in Sections J2.4(a), J2.4(b) and J2.4(c).

Sections J2.4(a) and J2.4(c) now require that the weld group has a uniform leg size.

A new equation, J2-7, has been provided for use in determining the nominal moment capacity of weld elements within a weld group when analyzed using the instantaneous center of rotation method.

TABLE J2.5
Available Strength of Welded Joints, ksi (MPa)

For PJP groove weld connections subjected to tension normal to the weld axis, the nominal strength of the base material has been altered in Table J2.5 to account for the removal of yielding as an applicable limit state and the corresponding resistance and safety factors have been changed.

J2.5. Combination of Welds

No changes have been made to this section.

J2.6. Filler Metal Requirements

No changes have been made to this section.

J2.7. Mixed Weld Metal

No changes have been made to this section.

J3. BOLTS AND THREADED PARTS

J3.1. High-Strength Bolts

High-strength bolts have been grouped according to material strength. Group A bolts are equivalent to A325 bolts, and Group B bolts are equivalent to A490 bolts. This grouping permits a simplification in the presentation of the provisions throughout Section J3.

For clarity, the exceptions to use of bolts in snug-tight connections are now presented. The definition of the snug-tight condition has been simplified, and a requirement that any bolts to be tightened to other than snug-tight be identified on the design drawings has replaced a requirement that all snug-tight bolts be identified.

A user note has been added to this section stating that there are no specific minimum or maximum tension requirements for snug-tight bolts and that fully pretensioned bolts such as ASTM F1852 or F2280 are permitted unless specifically prohibited on design drawings.

For clarity, the requirements relating to bolt geometry, such as for length and diameter, now refer to the 2009 RCSC *Specification*.

The conditions under which a single, hardened washer conforming to ASTM F436 shall be used in lieu of the standard washer and its associated user note have been moved to Section J3.2 in the 2010 *Specification*.

The paragraph referencing Section J3.10 for the provisions for adequate available bearing strength in slip-critical connections has been removed.

TABLE J3.1 and J3.1M
Minimum Bolt Pretension

No changes have been made in these tables.

TABLE J3.2
Nominal Strength of Fasteners and Threaded Parts, ksi (MPa)

The strength values for shear have been increased approximately 12.5%.

Several of the footnotes have been changed.

- For clarity, footnote [a] now applies to the entire "Nominal Tensile Strength" column.
- Footnote [b] addresses the influence of connection length effects and has been changed to correspond to the increase in shear strength values provided in the table. This had been footnote [f].
- Footnote [c] was footnote [b]. It now applies only when determining nominal shear strength.
- Footnote [d] was footnote [c].
- Footnote [d] in the 2005 *Specification* has been removed.
- Footnote [e] in the 2005 *Specification* has been incorporated into footnote [a].

J3.2. Size and Use of Holes

This section has been expanded to include the conditions under which a single, hardened washer is to be used, and its associated user note has been moved to this section from Section J3.1.

TABLE J3.3
Nominal Hole Dimensions

No changes have been made in this table.

J3.3. Minimum Spacing

A user note has been added to this section stating that ASTM F1554 anchor rods may be furnished in accordance to product specifications with a body diameter less than the nominal diameter.

J3.4. Minimum Edge Distance

No changes have been made to this section.

TABLE J3.4 and TABLE J3.4M
Minimum Edge Distance from Center of Standard Hole to Edge of Connected Part

Footnotes [c] and [d] have been removed because these limits are simply workmanship standards.

TABLE J3.5 and J3.5M
Values of Edge Distance Increment C_2

No changes have been made in these tables.

J3.5. Maximum Spacing and Edge Distance

A user note has been added to this section indicating that the requirements do not apply to elements consisting of two shapes in continuous contact.

J3.6. Tensile and Shear Strength of Bolts and Threaded Parts

The reference to footnote [d] of Table J3.2 has been removed from the definition of A_b because the footnote has been removed from the table.

A user note has been added to provide a conservative interpretation for determining the strength of a bolt group.

J3.7. Combined Tension and Shear in Bearing-Type Connections

This section was edited for clarity.

In the user note, the upper limit for when the provisions need not apply was corrected from 20% to 30% to be consistent with the equations provided.

J3.8. High-Strength Bolts in Slip-Critical Connections

The provisions for slip-critical connections have been completely revised. There is no longer a requirement that they be assessed under a serviceability limit.

- The equation for determining strength of bolts in slip-critical connections has been revised.

- The factor for hole type has been replaced by resistance and safety factors that vary depending on hole type.
- The mean slip coefficient for Class A surfaces has been reduced to 0.30.
- A fill factor has been added to account for the presence of more than one filler in a slip plane.

J3.9. Combined Tension and Shear in Slip-Critical Connections

This section has been edited for clarity.

J3.10. Bearing Strength at Bolt Holes

This section has been edited for clarity.

A user note has been added to provide a conservative interpretation for determining the strength of a bolt group.

J3.11. Special Fasteners

No changes have been made to this section.

J3.12. Tension Fasteners

No changes have been made to this section.

J4. AFFECTED ELEMENTS OF MEMBERS AND CONNECTING ELEMENTS

J4.1. Strength of Elements in Tension

A user note has been added to this section stating that the effective net area of the connection plate may be limited due to stress distribution as calculated by methods such as the Whitmore Section.

J4.2. Strength of Elements in Shear

No changes have been made to this section.

J4.3. Block Shear Strength

No changes have been made to this section.

J4.4. Strength of Elements in Compression

No changes have been made to this section.

J4.5. Strength of Elements in Flexure (new section)

This section identifies the limit states that must be checked for elements in flexure.

J5. FILLERS

For clarity, this section has been reorganized into four subsections.

J5.1. Fillers in Welded Connections (new section)

The requirements to which fillers and their connecting welds must conform have been established.

J5.1a. Thin Fillers (new section)

It has been clarified that thin fillers are not to be used to transfer stress; otherwise, no changes have been made in these requirements.

J5.1b. Thick Fillers (new section)

No changes have been made to these requirements.

J5.2. Fillers in Bolted Connections (new section)

A minimum reduction of 0.85 has been established for bolt shear strength with thick fills.

J6. SPLICES

No changes have been made to this section.

J7. BEARING STRENGTH

No changes have been made to this section.

J8. COLUMN BASES AND BEARING ON CONCRETE

The resistance and safety factors have been changed to be consistent with ACI 318.

J9. ANCHOR RODS AND EMBEDMENTS

For clarity, ACI 318 and 349 are now specified for the design of column bases and anchor rods when the transfer of forces to a concrete foundation is through bearing.

A user note has been added that recommends consideration of bearing on concrete for the transfer of horizontal forces at a base plate.

J10. FLANGES AND WEBS WITH CONCENTRATED FORCES

J10.1. Flange Local Buckling

No changes have been made to this section.

J10.2. Web Local Buckling

No changes have been made to this section.

J10.3. Web Local Crippling

No changes have been made to this section.

J10.4. Web Sidesway Buckling

No changes have been made to this section.

J10.5. Web Compression Buckling

No changes have been made to this section.

J10.6. Web Panel Zone Shear

This section has been edited for clarity.

J10.7. Unframed Ends of Beams and Girders

No changes have been made to this section.

J10.8. Additional Stiffener Requirements for Concentrated Forces

For clarity, references to the appropriate sections in J4 have been made for tension and compression stiffeners.

The requirement for the minimum stiffener thickness has been slightly modified.

J10.9. Additional Doubler Plate Requirements for Concentrated Forces

No changes have been made to this section.

CHAPTER K
DESIGN OF HSS AND BOX MEMBER CONNECTIONS

The major changes to this chapter include:

- The entire chapter is reorganized so that the requirements are presented in tabular form.
- Illustrations are included for the connection types associated with the specific requirements.
- The preamble has been edited for clarity, and user notes have been added.
- Section K4, “Welds of Plates and Branches to Rectangular HSS,” has been added.

K1. CONCENTRATED FORCES ON HSS

The limits of applicability that were listed in Section K1.2 in the 2005 *Specification* are now tabulated in Table K1.1A for round HSS and Table K1.2A for rectangular HSS.

All user notes from the 2005 *Specification* have been removed from this section.

K1.1. Definitions of Parameters

Variables A_g, F_c, S and l_b were added; variable N was removed; and some definitions were edited for clarity.

K1.2. Round HSS

The provisions are now presented in Tables K1.1 and K1.1A.

K1.3. Rectangular HSS

The provisions are now presented in Tables K1.2 and K1.2A.

K2. HSS-TO-HSS TRUSS CONNECTIONS

K2.1. Definitions of Parameters

Symbols have been edited for clarity.

K2.2. Round HSS

The provisions are now presented in Tables K2.1 and K2.1A.

K2.3. Rectangular HSS

The provisions are now presented in Tables K2.2 and K2.2A.

K3. HSS-TO-HSS MOMENT CONNECTIONS

K3.1. Definitions of Parameters

No changes have been made to this section.

K3.2. Round HSS

The provisions are now presented in Tables K3.1 and K3.1A.

K3.3. Rectangular HSS

The provisions are now presented in Tables K3.2 and K3.2A.

K4. WELDS OF PLATES AND BRANCHES TO RECTANGULAR HSS (new section)

Effective weld properties are established for use in determination of weld strength accounting for nonuniformity of load transfer along the weld length.

CHAPTER L
DESIGN FOR SERVICEABILITY

No major changes have been made to this chapter.

L1. GENERAL PROVISIONS

The user note has been edited for clarity.

L2. CAMBER

The user note has been removed.

L3. DEFLECTIONS

No changes have been made to this section.

L4. DRIFT
No changes have been made to this section.

L5. VIBRATION
No changes have been made to this section.

L6. WIND-INDUCED MOTION
No changes have been made to this section.

L7. EXPANSION AND CONTRACTION
No changes have been made to this section.

L8. CONNECTION SLIP
This section has been edited for clarity.

CHAPTER M
FABRICATION AND ERECTION

The major changes to this chapter include:

- Section M5, "Quality Control," has been relocated to new Chapter N, where it has been expanded.

M1. SHOP AND ERECTION DRAWINGS
This section has been edited for clarity to indicate that shop and erection drawings may be prepared in stages.

M2. FABRICATION

M2.1. Cambering, Curving and Straightening
No changes have been made to this section.

M2.2. Thermal Cutting
Requirements for reentrant corners have been expanded, and a user note has been added.

The requirement for crack inspections in accordance with ASTM E709 has been removed.

The user note has been revised to change the sample reference.

M2.3. Planing of Edges
No changes have been made to this section.

M2.4. Welded Construction
No changes have been made to this section.

M2.5. Bolted Construction
Water-jet cut holes are now permitted.

A user note has been added that provides a guide for evaluating the surface roughness of thermally cut holes.

M2.6. Compression Joints
No changes have been made to this section.

M2.7. Dimensional Tolerances
This section has been edited for clarity.

M2.8. Finish of Column Bases
No changes have been made to this section.

M2.9. Holes for Anchor Rods

No changes have been made to this section.

M2.10. Drain Holes

No changes have been made to this section.

M2.11. Requirements for Galvanized Members

This user note has been edited for clarity.

M3. SHOP PAINTING

M3.1. General Requirements

This section has been edited for clarity.

M3.2. Inaccessible Surfaces

No changes have been made to this section.

M3.3. Contact Surfaces

No changes have been made to this section.

M3.4. Finished Surfaces

No changes have been made to this section.

M3.5. Surfaces Adjacent to Field Welds

No changes have been made to this section.

M4. ERECTION

M4.1. Column Base Setting

This section has been edited for clarity.

M4.2. Stability and Connections

The title of this section has been changed from "Bracing." The requirement that the structure be secured to support dead, erection and other loads anticipated to occur as erection progresses has been moved here from Section M4.7, and that section has been deleted.

M4.3. Alignment

No changes have been made to this section.

M4.4. Fit of Column Compression Joints and Base Plates

No changes have been made to this section.

M4.5. Field Welding

This section has been edited for clarity and simplified.

M4.6. Field Painting

No changes have been made to this section.

CHAPTER N (new chapter)
QUALITY CONTROL AND QUALITY ASSURANCE

This chapter is new to the 2010 *Specification*. It addresses minimum requirements for quality control, quality assurance and nondestructive testing for structural steel systems and steel elements of composite members for buildings and other structures.

This chapter replaces Section M5 of the 2005 *Specification*.

N1. SCOPE (new section)
Quality control and quality assurance are defined.

N2. FABRICATOR AND ERECTOR QUALITY CONTROL PROGRAM (was Section M5)
The first sentence of the preamble to Section M5 of the 2005 *Specification* has been moved to this section, and it has been expanded to include minimum requirements for what the quality control inspector must inspect.

N3. FABRICATOR AND ERECTOR DOCUMENTS (new section)

N3.1. Submittals for Steel Construction
Documents to be submitted by the fabricator or erector are identified.

N3.2. Available Documents for Steel Construction
Documents to be available in electronic or printed form are identified.

N4. INSPECTION AND NONDESTRUCTIVE TESTING PERSONNEL (new section)

N4.1. Quality Control Inspector Qualifications
Qualifications are established for quality control welding inspection personnel.

N4.2. Quality Assurance Inspector Qualifications
Qualifications are established for quality assurance welding inspectors.

N4.3. NDT Personnel Qualifications
Qualifications are established for nondestructive testing personnel.

N5. MINIMUM REQUIREMENTS FOR INSPECTION OF STRUCTURAL STEEL BUILDINGS (new section)

N5.1. Quality Control
This new section identifies the quality control inspection tasks to be performed by the fabricator's or erector's quality control inspector.

N5.2. Quality Assurance
This new section identifies the quality assurance inspection tasks.

N5.3. Coordinated Inspection
This new section permits coordinated inspection between the quality control inspector and the quality assurance inspector.

N5.4. Inspection of Welding
Section M5.3 of the 2005 *Specification* has been moved to this section, and it has been expanded.
The first paragraph of Section M5.3 of the 2005 *Specification* is now a user note in this section.

N5.5. Nondestructive Testing of Welded Joints

N5.5a. Procedures
This new section identifies tests to be performed by quality assurance in accordance with AWS D1.1/D1.1M.

N5.5b. CJP Groove Weld NDT
This new section defines ultrasonic testing procedures for CJP groove welds.

N5.5c. Access Hole NDT
This new section specifies requirements for testing of weld access holes.

N5.5d. Welded Joints Subjected to Fatigue

This new section specifies requirements for weld soundness inspection.

N5.5e. Reduction of Rate of Ultrasonic Testing

This new section identifies when the rate of ultrasonic testing may be reduced.

N5.5f. Increase in Rate of Ultrasonic Testing

This new section identifies when the rate of ultrasonic testing must be increased.

N5.5g. Documentation

This new section specifies that all NDT performed shall be documented.

N5.6. Inspection of High-Strength Bolting

Section M5.4 of the 2005 *Specification* has been moved to this section, and it has been expanded.

N5.7. Other Inspection Tasks

This new section identifies what the fabricator's and erector's quality control personnel shall inspect and the documents to be used to verify compliance.

N6. MINIMUM REQUIREMENTS FOR INSPECTION OF COMPOSITE CONSTRUCTION (new section)

This new section identifies the tasks associated with inspection of structural steel and steel deck used in composite construction.

N7. APPROVED FABRICATORS AND ERECTORS (new section)

This new section specifies when quality assurance inspections may be waived for approved fabricators and erectors.

N8. NONCOMFORMING MATERIAL AND WORKMANSHIP (new section)

Section M5.2 of the 2005 *Specification* has been moved to this section, and it has been expanded to include instructions on dealing with nonconforming material.

APPENDIX 1
DESIGN BY INELASTIC ANALYSIS

The major changes to this appendix include:

- How to design using inelastic analysis has been clarified.
- The negative moment redistribution provisions have been relocated to Sections B3.7 and F13.5.
- The appendix has been reorganized into three new sections.

1.1 GENERAL REQUIREMENTS (new section)

Sections 1.8 and 1.9 of the 2005 *Specification* have been moved here and expanded. The requirements for inelastic analysis have been defined, and the basic procedure for performing an inelastic analysis have been outlined.

1.2 DUCTILITY REQUIREMENTS (new section)

1.2.1. Material

Section 1.2 of the 2005 *Specification* has been moved to this section and edited for clarity.

1.2.2. Cross Section

Section 1.4 of the 2005 *Specification* has been moved to this section. The controlling width-to-thickness ratio, λ_{pd}, is defined.

1.2.3. Unbraced Length

Section 1.7 of the 2005 *Specification* has been moved to this section, and the equations have been modified.

A third case, tension only, has been defined where there is no L_{pd} limit.

1.2.4. Axial Force

This section is based on Section 1.5.2 of the 2005 *Specification* and requires that the compressive design strength for compression members with plastic hinges not exceed $0.75F_yA_g$.

1.3 ANALYSIS REQUIREMENTS (new section)

1.3.1. Material Properties and Yield Criteria

This section provides requirements previously specified in Sections 1.5, 1.6, 1.7 and 1.8 of the 2005 *Specification*.

1.3.2. Geometric Imperfections

This section requires that initial geometric imperfections be taken into account during an inelastic analysis.

1.3.3. Residual Stress and Partial Yielding Effects

This section requires that the effect of residual stresses and partial yielding be part of the inelastic analysis.

APPENDIX 2
DESIGN FOR PONDING

No major changes have been made in this appendix.

2.1. SIMPLIFIED DESIGN FOR PONDING

This section has been edited for clarity.

2.2. IMPROVED DESIGN FOR PONDING

This section has been edited for clarity.

APPENDIX 3
DESIGN FOR FATIGUE

No major changes have been made in this appendix.

3.1. GENERAL PROVISIONS

The conditions under which evaluation of fatigue resistance is not required have been expanded.

3.2. CALCULATION OF MAXIMUM STRESSES AND ALLOWABLE STRESS RANGES

No changes have been made to this section.

3.3. PLAIN MATERIAL AND WELDED JOINTS

This section has been edited for clarity.

3.4. BOLTS AND THREADED PARTS

The factors C_f and F_{TH} are now provided in Table A-3.1.

3.5. SPECIAL FABRICATION AND ERECTION REQUIREMENTS

This section requires that longitudinal backing, if left in place, be attached with continuous fillet welds.

A user note has been added indicating that AWS C4.1 Sample 3 may be used to evaluate compliance with these requirements.

TABLE A-3.1
Fatigue Design Parameters

The table has been edited and additional figures included for clarity. Additional changes include:

- The thickness criteria for determining C_f and F_{TH} have been changed.
- Weld soundness must be established by radiographic or ultrasonic inspection in accordance with the requirements of subclauses 6.12 or 6.13 of AWS D1.1/D1.1M.
- The provisions for selecting stress categories E and E′ have changed.

APPENDIX 4
STRUCTURAL DESIGN FOR FIRE CONDITIONS

The major change in this appendix includes:

- The strength equations for compression and flexure when using the "Simple Methods of Analysis" have been revised.

4.1. GENERAL PROVISIONS

Terms that were defined in this section in the 2005 *Specification* have been moved to the Glossary.

4.1.1. Performance Objective

No changes have been made to this section.

4.1.2. Design by Engineering Analysis

It is now required that load and resistance factor design be used for structural design for fire conditions.

4.1.3. Design by Qualification Testing

No changes have been made to this section.

4.1.4. Load Combinations and Required Strength

This section has been edited for clarity.

4.2. STRUCTURAL DESIGN FOR FIRE CONDITIONS BY ANALYSIS

4.2.1. Design-Basis Fire

No changes have been made to this section.

4.2.1.1. Localized Fire

No changes have been made to this section.

4.2.1.2. Post-Flashover Compartment Fires

Section 4.2.1.4, "Fire Duration," from the 2005 *Specification* has been moved to this section.

4.2.1.3. Exterior Fires

No changes have been made to this section.

4.2.1.4. Active Fire Protection System (was Appendix 4, Section 2.1.5)

No changes have been made to this section.

4.2.2. Temperatures in Structural Systems Under Fire Conditions

No changes have been made to this section.

4.2.3. Material Strengths at Elevated Temperatures

No changes have been made to this section.

4.2.3.1. Thermal Elongation

No changes have been made to this section.

4.2.3.2. Mechanical Properties at Elevated Temperatures

The proportional limit at elevated temperatures, $F_p(T)$, and the shear modulus, G, are now defined.

TABLE A-4.2.1
Properties of Steel at Elevated Temperatures

The proportional limit coefficient and the relationship for shear modulus at elevated temperatures are now given in this table.

TABLE A-4.2.2
Properties of Concrete at Elevated Temperatures

The subheading for $\varepsilon_{cu}(T)$ has been corrected to normal-weight concrete.

4.2.4. Structural Design Requirements

4.2.4.1. General Structural Integrity

No changes have been made to this section.

4.2.4.2. Strength Requirements and Deformation Limits

No changes have been made to this section.

4.2.4.3. Methods of Analysis

4.2.4.3a. Advanced Methods of Analysis

No changes have been made to this section.

4.2.4.3b. Simple Methods of Analysis

It is now stated that temperature effects for steel temperatures less than or equal to 400 °F need not be considered in calculating member strengths.

(1) Tension Members

No changes have been made to this section.

(2) Compression Members

A new compression strength equation has been provided.

(3) Flexural Members

New flexural strength equations have been provided.

(4) Composite Floor Members

No changes have been made to this section.

4.2.4.4. Design Strength

No changes have been made to this section.

4.3. DESIGN BY QUALIFICATION TESTING

4.3.1. Qualification Standards

No changes have been made to this section.

4.3.2. Restrained Construction

No changes have been made to this section.

4.3.3. Unrestrained Construction

No changes have been made to this section.

APPENDIX 5
EVALUATION OF EXISTING STRUCTURES

No changes have been made to this appendix.

APPENDIX 6
STABILITY BRACING FOR COLUMNS AND BEAMS

The major changes to this appendix include:

- The addition of Section 6.4, with provisions for beam-column bracing.
- The addition of a user note to provide definitions for relative and nodal braces.

6.1. GENERAL PROVISIONS

This section has been edited for clarity and expanded.

The definitions of "relative brace" and "nodal brace" have been moved to a new user note.

6.2. COLUMN BRACING

6.2.1. Relative Bracing

No changes have been made to this section.

6.2.2. Nodal Bracing

This section has been edited for clarity.

6.3. BEAM BRACING

This section has been edited for clarity.

6.3.1. Lateral Bracing

This section has been edited for clarity.

6.3.1a. Relative Bracing

This section has been edited for clarity.

6.3.1b. Nodal Bracing

No changes have been made to this section.

6.3.2. Torsional Bracing

This section has been edited for clarity.

6.3.2a. Nodal Bracing

This section has been edited for clarity.

6.3.2b. Continuous Bracing

This section has been edited for clarity.

6.4. BEAM-COLUMN BRACING (new section)

This section provides the requirements for combining strength and stiffness for beam-columns.

APPENDIX 7
ALTERNATIVE METHODS OF DESIGN FOR STABILITY

This appendix has been renamed and reorganized as follows:

- The title of this appendix has been changed from "Direct Analysis Method to Alternative Methods of Design for Stability." This reflects the fact that the direct analysis method has been moved to Chapter C, and the effective length method and first-order analysis method have been moved from Chapter C to this appendix.
- The titles of Sections 7.2 and 7.3 have been changed from "Notional Loads and Design-Analysis Constraints to Effective Length Method" and "First-Order Analysis Method," respectively.
- The presentation of these two alternative methods has been reorganized for clarity.

7.1. GENERAL STABILITY REQUIREMENTS

Sections C1 and C2 are incorporated by reference, and the effective length method and first-order analysis method are introduced. The effective length method was formerly called the second-order analysis method.

7.2. EFFECTIVE LENGTH METHOD

7.2.1. Limitations

The parts of Section C2.2 of the 2005 *Specification* that reference the effective length method have been moved here and edited for clarity.

The 1.6 factor for ASD load combinations has been removed from the user note and has been placed in a list of conditions in this section.

7.2.2. Required Strengths

The parts of Section C2.2 of the 2005 *Specification* that reference the effective length method have been moved here and edited for clarity.

A user note has been added that explains why the notional load need only be applied in gravity-only load cases.

7.2.3. Available Strengths

Sections C1.3a, C1.3b and C1.3c of the 2005 *Specification* have been moved to this section and represent the provisions for determining the effective length factor, K.

7.3. FIRST-ORDER ANALYSIS METHOD

7.3.1. Limitations

The limitations in this section have been moved from Section C2.2 and Section C2.2b of the 2005 *Specification*.

7.3.2. Required Strengths

Section C2.2b of the 2005 *Specification* has been moved to this section.

The equation for notional load has been slightly modified for clarity.

7.3.3. Available Strengths

The first two paragraphs of Section C1.2 of the 2005 *Specification* have been moved to this section.

A user note referencing Appendix 6 for methods of satisfying bracing requirements has been added.

APPENDIX 8 (new appendix)
APPROXIMATE SECOND-ORDER ANALYSIS

This appendix is new to the 2010 *Specification*. The approximate second-order analysis method (the B_1-B_2 method) has been moved from Chapter C.

8.1. LIMITATIONS (new section)
This section states the limitations of the procedure.

8.2. CALCULATION PROCEDURE (was Section C2.1b)
This section has been edited for clarity.

8.2.1. Multiplier B_1 for P-δ Effects
This section has been edited for clarity.

8.2.2. Multiplier B_2 for P-Δ Effects
This section has been edited for clarity. In addition, a new equation has been provided to address distribution of load on moment frame and gravity-only columns.

REFERENCES

AISC (2005), *Specification for Structural Steel Buildings*, March 9, American Institute of Steel Construction, Chicago, IL.

AISC (2010), *Code of Standard Practice for Steel Buildings and Bridges*, April 14, American Institute of Steel Construction, Chicago, IL.

AISC (2010), *Seismic Provisions for Structural Steel Buildings*, AISC 341-10, American Institute of Steel Construction, Chicago, IL.

AISC (2010), *Specification for Structural Steel Buildings*, June 22, American Institute of Steel Construction, Chicago, IL.

AISC (2011), *Steel Construction Manual*, 14th ed., American Institute of Steel Construction, Chicago, IL.

Brockenbrough, R.L. (2002), *AISC Rehabilitation and Retrofit Guide—A Reference for Historical Shapes and Specifications*, Design Guide 15, AISC, Chicago, IL.

GUIDE FOR AUTHORS

SCOPE: The ENGINEERING JOURNAL is dedicated to the improvement and advancement of steel construction. Its pages are open to all who wish to report on new developments or techniques in steel design, research, the design and/or construction of new projects, steel fabrication methods, or new products of significance to the uses of steel in construction. Only original papers should be submitted.

GENERAL: Papers intended for publication may be submitted by mail to the Editor, Keith Grubb, ENGINEERING JOURNAL, AMERICAN INSTITUTE OF STEEL CONSTRUCTION, One East Wacker Drive, Suite 700, Chicago, IL, 60601, or by email to grubb@aisc.org.

The articles published in the *Engineering Journal* undergo peer review before publication for (1) originality of contribution; (2) technical value to the steel construction community; (3) proper credit to others working in the same area; (4) prior publication of the material; and (5) justification of the conclusion based on the report.

All papers within the scope outlined above will be reviewed by engineers selected from among AISC, industry, design firms, and universities. The standard review process includes outside review by an average of three reviewers, who are experts in their respective technical area, and volunteers in the program. Papers not accepted will not be returned to the author. Published papers become the property of the American Institute of Steel Construction and are protected by appropriate copyrights. No proofs will be sent to authors. Each author receives three copies of the issue in which his contribution appears.

MANUSCRIPT PREPARATION: Manuscripts must be provided in Microsoft Word format. Include a PDF with your submittal. View our complete author guidelines at **www.aisc.org/ej**.

There's always a solution in steel.

ENGINEERING JOURNAL
American Institute of Steel Construction
One East Wacker Drive, Suite 700
Chicago, IL 60601

312.670.2400 www.aisc.org